An endophytic Fusarium–legume association is partially dependent on the common symbiotic signalling pathway

DR PAOLA BONFANTE (Orcid ID : 0000-0003-3576-8530)

PROF. KALLIOPE K PAPADOPOULOU (Orcid ID : 0000-0001-7731-1825)

Article type : Regular Manuscript

An endophytic *Fusarium*-legume association is partially dependent on the common symbiotic signalling pathway

Vasiliki Skiada[1], Marianna Avramidou[1], Paola Bonfante[2], Andrea Genre[2], Kalliope K. Papadopoulou[1*]

[1] Department of Biochemistry and Biotechnology, University of Thessaly, Biopolis, Larissa, 41500, Greece

[2] Department of Life Sciences and Systems Biology, University of Torino, Torino, 10125, Italy

Corresponding author

Kalliope K. Papadopoulou

Department of Biochemistry and Biotechnology, School of Health Sciences, University of Thessaly, Biopolis, Larissa, 41500, Greece

Phone: +30 2410 565244, E-mail: kalpapad@bio.uth.gr

Received: 4 October 2019

Accepted: 21 January 2020

ORCID

Vasiliki Skiada https://orcid.org/0000-0003-4084-4120

Marianna Avramidou https://orcid.org/0000-0002-4023-6750
Paola Bonfante https://orcid.org/0000-0003-3576-8530
Andrea Genre https://orcid.org/0000-0001-5029-6194
Kalliope K. Papadopoulou https://orcid.org/0000-0001-7731-1825

Total word count (main body): 7414
Word count (Summary): 165 , Word count (Introduction): 905
Word count (Materials and Methods): 1270, Word count (Results): 2393
Word count (Discussion): 2681
Figures in black and white: 1
Figures in colour: 5
Supplementary Methods: 1
Supplementary Figures: 10
Supplementary Tables: 2

Summary

- Legumes interact with a wide range of microbes in their root system, ranging from beneficial symbionts to pathogens. Symbiotic rhizobia and arbuscular mycorrhizal glomeromycetes trigger a so-called common symbiotic signalling pathway (CSSP), including the induction of nuclear calcium spiking in the root epidermis.
- By combining gene expression analysis, mutant phenotypic screening, and analysis of nuclear calcium elevations, we demonstrate that recognition of an endophytic *Fusarium solani* strain K (FsK) in model legumes initiates via perception of chitooligosaccharidic molecules and is, at least partially, CSSP-dependent.
- FsK induced the expression of Lysin-motif receptors for chitin-based molecules, CSSP members and CSSP-dependent genes in *Lotus japonicus*. In *LysM* and CSSP mutant/RNAi lines, root penetration and fungal intraradical progression was either stimulated or limited, while FsK exudates triggered CSSP-dependent nuclear calcium spiking, in epidermal cells of *Medicago truncatula* Root Organ Cultures.
- Our results corroborate that the CSSP is involved in the perception of signals from other microbes beyond the restricted group of symbiotic interactions *sensu stricto*.

Keywords: calcium spiking, chitooligosaccharides, endophytism, *Fusarium*, *Lotus japonicus*, *Medicago truncatula*, symbiosis

Introduction

Plants encounter diverse microorganisms at the root-soil interface, some of which invade the root system and establish detrimental or beneficial associations (Zipfel & Oldroyd, 2017). In this scenario, legumes are unique in their ability to establish two types of mutualistic symbioses: the arbuscular mycorrhizal (AM) and rhizobium-legume (RL) symbiosis. For both interactions, a few plant-directed microbial signals have been characterized so far, and all of them are water soluble chitin-based molecules. Rhizobia produce Nod Factors (NFs), lipo-chitooligosaccharides (LCOs) that are recognized by specific receptor-like kinases (RLKs) (Amor *et al.*, 2003) (Limpens *et al.*, 2003) (Madsen *et al.*, 2003) (Murakami *et al.*, 2018) (Radutoiu *et al.*, 2003), whereas AM fungi release both Nod factor-like Myc-LCOs (Maillet *et al.*, 2011) and short-chain chitin oligomers (Myc-COs) (Genre *et al.*, 2013). The perception of chitin-related molecules in plants is mediated by Lysin-motif (LysM)-RLKs (Antolín-Llovera *et al.*, 2014). This is also the case for Nod factors and Myc-LCOs (Fliegmann et al., 2013) (Maillet et al., 2011), whereas specific receptors for Myc-COs in legumes remain to be characterized, as no clear AM phenotype in corresponding mutants have been recorded.

Downstream of receptor activation, the intracellular accommodation of both types of symbionts is mediated by a so-called common symbiosis signalling pathway (CSSP) that in *Lotus japonicus* (*Lj*) includes eight genes: the plasma membrane (PM)-bound RLK *Lj*SYMRK (*Mt*DMI2 in *Medicago truncatula, Mt*); three nucleoporins (NUP85, NUP133, NENA); the nuclear envelope located cation channels *Lj*CASTOR, and *Lj*POLLUX (*Mt*DMI1, orthologous to POLLUX), with

LjCASTOR recently reported to act as highly selective Ca^{2+} channel (Kim *et al.*, 2019); the nuclear calcium and calmodulin-dependent protein kinase *Lj*CCaMK (*Mt*DMI3), the CCaMK phosphorylation substrate *Lj*CYCLOPS (Kistner *et al.*, 2005) (Charpentier *et al.*, 2008) (Genre & Russo, 2016). Downstream the CSSP lie nodulation/mycorrhization specific transcription factors such as *Lj*NSP1 and *Lj*NSP2 (Catoira *et al.*, 2000) (Delaux *et al.*, 2013) (Kalo *et al.*, 2005) (Maillet *et al.*, 2011), and early nodulin genes, like *LjENOD2* and *LjENOD40* (Glyan'ko, 2018) (Ferguson & Mathesius, 2014) (Takeda *et al.*, 2005). A central element of the CSSP is the triggering of repeated oscillations in nuclear calcium concentration (spiking). In fact, mutants in all CSSP members acting upstream of CCaMK are defective for calcium spiking (Harris *et al.*, 2003) (Miwa *et al.*, 2006) (Parniske, 2008), and the nuclear-localized CCaMK is considered to act as a decoder of the calcium signal, which is translated into phosphorylation events (Yano *et al.*, 2008). Consequently, the induction of nuclear calcium spiking has been used as a reliable reporter of CSSP activation by symbiotic microbes or their isolated signals (Wais *et al.*, 2000) (Sieberer *et al.*, 2009) (Chabaud *et al.*, 2011) (Genre *et al.*, 2013) (Charpentier & Oldroyd, 2013). In particular, this approach has been applied in studies of AM fungal signalling in both legume and non-legume hosts, using either whole plants or root organ cultures (ROCs) expressing nuclear-localized, calcium-sensing reporters, such as cameleon proteins (Chabaud *et al.*, 2011) (Genre *et al.*, 2013) (Sun *et al.*, 2015) (Carotenuto *et al.*, 2017).

Fusarium solani strain K (FsK) is a beneficial endophytic isolate of tomato, protecting the plant against root and foliar pathogens (Kavroulakis *et al.*, 2007), spider mites (Pappas *et al.*, 2018), zoophytophagous insects (Garantonakis *et al.*, 2018), and drought (Kavroulakis *et al.*, 2018). We have recently shown that FsK efficiently colonizes legume roots and demonstrates plasticity throughout colonization (Skiada *et al.*, 2019). Early FsK colonization of legume roots triggers a number of host cell responses (i.e. cytoplasm/ER accumulation, nuclear movement, membrane trafficking at contact sites) known to also occur in both symbiotic and pathogenic interactions (Genre *et al.*, 2009) (Skiada *et al.*, 2019). We were in particular interested in investigating the molecular factors that mediate the accommodation of this endophytic ascomycetous fungus. The availability of biological tools developed to decipher the establishment of symbionts within legume plant tissues, prompted us to investigate the role of the CSSP in the FsK endophytic legume association.

A role for the CSSP in non-symbiotic interactions, has been investigated by many research groups: some propose an (at least partial) involvement (Sanchez *et al.*, 2005) (Weerasinghe *et al.*, 2005)

(Fernandez-Aparicio *et al.*, 2010) (Wang *et al.*, 2012) (Zgadzaj *et al.*, 2015) (Thiergart *et al.*, 2019), while others do not (Banhara *et al.*, 2015) (Huisman *et al.*, 2015). Recently, a role for the CSSP in symbiotic associations of non-legume plants was demonstrated: LCOs produced by the ectomycorrhizal fungus *Laccaria bicolor* trigger nuclear Ca^{2+} spiking in the roots of *Populus*, and fungal colonization proceeded in a *CASTOR*/*POLLUX* and *CCaMK* dependent manner (Cope *et al.*, 2019). Nevertheless, neither a clear-cut demonstration of the induction of nuclear calcium spiking by non-symbiotic, endophytic microbial partners, nor a compromised colonization phenotype by a non-symbiont in a CSSP mutant, have thus far been reported.

In this work, we employed gene expression analysis and phenotypic screening of mutant/RNAi lines to investigate the role of certain *LysM* receptors in the *Lotus*-FsK interaction. We furthermore demonstrate that the expression of *L. japonicus* markers of AM and/or RL symbiosis is partially altered in the presence of FsK, while two CSSP mutants, *ccamk* and *cyclops,* display a compromised entry and delay in fungal colonization. Lastly, we show that the endophyte exudates triggered CSSP-dependent nuclear calcium spiking in the outer root tissues of *M. truncatula* ROCs, which is also observed for exudates from other root-interacting fungi. Overall, our results show that multiple *LysM* receptors participate in FsK recognition and suggest that the core of the CSSP is also involved in the perception of diffusible signals from non-mycorrhizal fungi.

Materials and methods

Plant material

L. japonicus wild-type (wt) plants and the CSSP mutant lines *symrk-1*, *castor-1*, *sym15-1 (ccamk-1), sym6-1* (*cyclops-1*), as well as the *LysM* mutant lines *lys6-1*, *lys12-3* and the triple mutant *nfr1nfr5lys11* were used for phenotypic screening of FsK intraradical abundance. All mutant lines were kindly provided by Associate Prof Simona Radutoiu (Department of Molecular Biology and Genetics - Plant Molecular Biology, Aarhus, Denmark). The plants were chemically scarified and grown in Petri dishes as described previously (Skiada *et al.*, 2019) until seedlings transplantation to magenta boxes.

L. japonicus wt plants (ecotype 'Gifu') were used for gene expression analysis experiments.

M. truncatula ROC lines and the CSSP mutant ROC lines *dmi2-2* and *dmi3-1*, expressing the 35S:NupYC2.1 construct (Sieberer *et al.*, 2009) were obtained previously (Chabaud *et al.*, 2011). An apical segment deriving from each ROC line was routinely transferred to square Petri dishes

containing M medium (Bécard & Fortin, 1988) (Chabaud *et al.*, 2002). Segments derived from ROCs were used for calcium spiking bioassays upon fungal exudates and chitooligosaccharide treatment.

Fungal material

Fusarium solani strain K (FsK) (Kavroulakis *et al.*, 2007) was routinely cultured as previously described (Skiada *et al.*, 2019). Fungal conidia were used as inoculum for phenotypic profiling of all mutant lines and for gene expression analysis experiments. *Fusarium oxysporum* f. sp. *medicaginis* (Fom, BPIC 2561) (Snyder & Hansen, 1940) was kindly provided by Benaki Phytopathological Institute (Benaki phytopathological Institute Collection, BPIC), Attiki, Greece. *Piriformospora indica* (MUT00004176) was kindly provided by Mycotheca Universitatis Taurinensis, Turin, Italy. FsK, Fom and *P. indica* hyphal propagules were used for preparation of fungal exudates for calcium spiking analyses.

Experimental setup for gene expression analysis and phenotypic screening of *L. japonicus* mutants

L. japonicus seedlings (7-11 days old) were transplanted into magenta boxes (3 plants per magenta) containing sterile sand:vermiculite (3:1) and directly inoculated on the root with 10^2 conidia per plant. Control plants received the same volume of sterile water. The substrate was watered with 30 ml of M medium (Boisson-Dernier et al., 2001) prior to transplantation, in both treatments. Magenta boxes were transferred in a growth chamber (16h light/8h dark photoperiod, 22°C).

For gene expression analysis, plants were harvested at 1, 2, 4, 6, 12 days post inoculation (dpi), washed 5x with sterile water to remove the excess extraradical mycelium, root tissues were collected, flash frozen under liquid nitrogen and kept at -80°C until subsequent DNA/RNA isolation. Four (4) biological replicates were assessed for each treatment, with each replicate consisting of 3 individual plants.

For phenotypic profiling, wt and CSSP mutants were harvested at 4 and 8 dpi and *LysM* mutants were harvested at 4 dpi. Different batches of wt *L. japonicus* plants were assessed for CSSP or for *LysM* mutants. Harvested plants were surface sterilized (1% v/v NaOCl for 1 min), washed 5x

with sterile water and prepared as above for DNA isolation. Five (5) biological replicates were assessed for each treatment, with each replicate consisting of 3 individual plants.

Agrobacterium rhizogenes-mediated hairy-root transformation

A 176 bp fragment specific of *Lys13*/*Lys14* genes (100% nucleic acid similarity in both genes) was amplified by PCR using specific primers (Table S2), and was introduced in the pUBI-GWS-GFP vector (Maekawa *et al.*, 2008). The binary vector was transformed into *Agrobacterium rhizogenes* LBA1334 and used for generation of *L. japonicus* hairy roots as described previously (Krokida *et al.*, 2013). Control plants were transformed with the empty pUBI-GWS-GFP vector.

Plants with regenerated hairy roots (16 days old) were transferred into pots containing sterile sand:vermiculite (3:1) substrate, in a growth chamber (16h light/8h dark photoperiod, 22°C).. Two days post transfer, plants were inoculated with 10^2 FsK conidia per root, and root tissues were harvested at 5 dpi for subsequent DNA/RNA isolation.

Silencing of *Lys13*, *Lys14* was verified by gene expression analysis. Based on these results 7 lines were chosen showing reduced expression levels of *Lys13*, *Lys14* or both. DNA was isolated from the same tissues and 1µl was used for estimation of intraradical fungal abundance.

Gene expression analysis – Quantification of fungal colonization

L. japonicus total DNA was isolated using the CTAB method (Doyle & Doyle, 1987). For quantification of intraradical fungal abundance, the weight of the plant tissue was determined prior to DNA isolation. DNA concentration was determined using Qubit 2.0 fluorometer. Total RNA was extracted using the Isolate II RNA Plant Kit (BIO-52077, BIOLINE, London, UK) according to manufacturer's instructions, and treated with DNase I (18047019, Invitrogen, Carlsbad, California, USA) at 37°C for 1h. First strand cDNA was synthesized using the PrimeScript™ 1st strand cDNA Synthesis Kit (6110A, Takara, Shiga, Japan). Quantitative real-time RT-PCR (qPCR) was performed using gene-specific primers (Table S2) as described in detail in Supporting Information (Methods S1).

To estimate fungal abundance within root tissues, absolute quantification of *F. solani ITS* or *TEF1a* gene was performed as described in (Skiada *et al.*, 2019). Details are provided in Methods S1.

Preparation of fungal exudates, COs solution, and root treatment

Exudates of FsK, Fom and *P. indica* were prepared as previously described (Lace *et al.*, 2015). Exudates of *Gigaspora margarita* were prepared as described in (Chabaud *et al.*, 2011). Detailed description of treatments of primary *Mt* wild type and *dmi2-2*/*dmi3-1* mutant ROCs with the exudates is provided in Methods S1.

Chitinase treatment of FsK, Fom exudate, and of pentameric chito-oligosaccharide (CO5) solution was performed using 1 mg ml^{-1} chitinase from *Streptomyces griseus* (ref C6137; Sigma-Aldrich, St. Louis, Missouri, USA) in sterile H_2O for 16 h at room temperature. Autoclave treatment was performed by autoclaving the fungal exudates (121 °C, 1 atm) for 20 min or for 1 h.

Confocal microscopy for calcium spiking measurements in *M. truncatula* ROC epidermis

A FRET-based ratiometric approach (Sieberer *et al.*, 2009) was used to record the relative changes of nuclear calcium concentrations corresponding to Yellow Fluorescent Protein (YFP) to Cyan Fluorescent Protein (CFP) fluorescence intensity changes over time (Miyawaki *et al.*, 1997). Analysis was performed using a Leica TCS SP2 confocal microscope fitted with a long distance x40 water-immersion objective (HCX Apo 0.80). Measurements were performed and settings were set as previously described (Chabaud *et al.*, 2011). The pinhole diameter was set at 6 airy units (AU). YFP and CFP fluorescence intensities were calculated for each region of interest (each nucleus) using Leica LCS software. Values were then exported to a Microsoft Excel spreadsheet, the YFP/CFP ratio for each time frame was calculated, and ratio values were plotted over time. Nuclear spiking was examined in all cases in an atrichoblast/low-trichoblast zone located 10-20 mm from the root tip.

Calcium spiking measurements were furthermore analyzed using CaSA software (Russo *et al.*, 2013). The generation of at least 3 peaks was the threshold for discrimination between responding and non-responding cells. CaSA output PNG image files, were used to manually calculate peak width and lag phases prior to calcium spiking response initiation in responding nuclei. CaSa output waiting time autocorrelation values were used to generate the corresponding histogram.

Statistical analysis

Two-way Anova followed by Tukey's post-hoc test was used in gene expression analysis data. Student's t-test was used in all pairwise comparisons. One-way Anova was used in comparisons between 3 or more independent (unrelated) groups (i.e. analysis of calcium spiking results obtained after plant cells elicitation with the three investigated fungal exudates). The non-

parametric Kolmogorov-Smirnov (K-S) two-sample test was used to assess whether data corresponding to a) number of peaks, b) lag phase prior to spiking initiation, c) width of peaks, generated in *Mt* nuclei by the 3 elicitors, are drawn from the same distribution (pairwise comparisons among results from the 3 elicitors). Pearson's chi squared test was used to test whether the frequency distribution of waiting times autocorrelation values of peaks generated by the 3 fungal exudates are independent. Statistical analyses used are indicated in detail in the corresponding Figures/Figure legends.

Results

FsK inoculation affects the expression of CSSP members and CSSP-regulated genes

Previously, we have shown that early FsK colonization of legume roots is accompanied by fungal plasticity and a number of host cell responses (Skiada *et al.*, 2019). This prompted us to investigate potential similarities with symbiosis-related plant gene expression. We, therefore, analyzed the expression of key CSSP components, such as *LjCASTOR*, *LjCCaMK* and *LjCYCLOPS*, as well as CSSP-regulated symbiosis markers, namely *LjNSP1*, *LjNSP2*, *LjIPN2*, *LjENOD40 and LjENOD2*. Their regulation was investigated at specific time points during *Lotus*-FsK interaction, alongside fungal colonization levels (Fig. S1, S2). The expression of *LjCCaMK* was marginally but significantly upregulated upon FsK inoculation at very early stages of the interaction (1 dpi), reaching a 2.2-fold upregulation compared to controls at 12 dpi. By contrast, no significant difference was recorded in the expression of *LjCASTOR* and *LjCYCLOPS*, or the transcription factors *LjNSP1* and *LjNSP2*, or *LjIPN2* (Interacting Protein of NSP2) acting downstream the CSSP, in control and inoculated plants at any time point (Fig. S1, S2).

We then tested whether the expression of the symbiosis marker gene *LjENOD40* was altered in our *Lotus*-FsK interaction system. We focused on *LjENOD40-1* gene, which is strongly upregulated at very early stages of rhizobium infection, in contrast to the mature nodule marker *LjENOD40-2* (Kumagai *et al.*, 2006). A statistically significant induction of *LjENOD40-1* was observed at 2, 4 and 6 dpi (1.6-, 1.9-, 1.7-fold, respectively) in inoculated compared to non-inoculated plants. *ENOD40* expression coincides with maximum levels of intraradical fungal accommodation (recorded at 4 dpi) (Fig. S2). By contrast, we recorded no differences between control and inoculated plants in the expression levels of our second nodulation marker gene, *ENOD2*, which is expressed in legumes during rhizobial and AM infection and nodule

morphogenesis, but not upon fungal pathogen infection (Franssen *et al.*, 1987) (van de Wiel *et al.*, 1990) (van Rhijn *et al.*, 1997).

To summarize, our analyses revealed that FsK colonization was associated with the upregulation of a subset of known symbiosis markers over the course of 12 days post inoculation.

FsK colonization is reduced in CSSP mutants compared to wt plants

Based on our gene expression results, we investigated the phenotypic differences in FsK colonization of *L. japonicus* CSSP mutants compared to wt plants (Fig. 1). We selected mutant lines impaired in CSSP genes acting upstream (*symRK-1*, *castor-1*) and downstream of nuclear calcium spiking (*ccamk-1*, *cyclops-1*). FsK intraradical colonization was quantified via qPCR at 4 and 8 dpi (Fig. 1b), when roots are well-colonized by the fungus under our experimental conditions (Fig. S2). The colonization of *symRK-1* and *castor-1* mutants was similar to that of wt plants. By contrast, a significant reduction in fungal colonization was observed in both *ccamk-1* (75.17%) and *cyclops-1* (68.82%) compared to wt plants at 4 dpi. A comparable reduction in fungal intraradical colonization persisted at 8 dpi only in *cyclops-1* plants (45.77%).

In conclusion, our phenotypic analysis revealed a significant reduction in FsK colonization only for CSSP mutants for genes that act downstream of nuclear calcium spiking, and the reduction was more evident at earlier time points of the interaction. This implies that the CSSP is necessary for proper colonization by FsK, though perhaps not the only route, as we did not record a complete abolishment in colonization levels in any of the mutants examined.

Fungal exudates trigger nuclear calcium spiking in wt *M. truncatula* ROC epidermis

Based on the colonization phenotype in CSSP mutant lines, we then investigated nuclear calcium signals in response to FsK exudate treatment. To this aim, we used wt *Medicago truncatula* ROCs expressing the nuclear localized cameleon reporters (NupYC2.1), thus allowing FRET based imaging analysis of nuclear calcium responses (Chabaud *et al.*, 2011) (Carotenuto *et al.*, 2019).

We focused on epidermal cells in an area 1-2 cm above the root tip harbouring few trichoblasts, because this root zone in model legumes is susceptible to colonization by FsK (Skiada *et al.*, 2019) and is also reported to show the strongest calcium spiking responses to AM fungal exudate (Chabaud *et al.*, 2011). As additional controls, we extended our analysis to include other compatible legume colonizers: the pathogenic *Fusarium oxysporum* f.sp. *medicaginis* (Snyder & Hansen, 1940), and *Piriformospora (Serendipita) indica* (Hayes *et al.*, 2014) (Ramírez-Suero *et*

al., 2010), an endophytic fungus with a versatile lifestyle, able to colonize *L. japonicus* CSSP mutant lines (Verma *et al.*, 1998) (Deshmukh *et al.*, 2006) (Lahrmann *et al.*, 2013) (Banhara *et al.*, 2015).

Exudates from all tested fungi triggered nuclear calcium oscillations in wt *M. truncatula* epidermal cells (Fig. 2, Fig. S3; control treatments are presented in Fig. S4, whereas details about the biological replicates and nuclei screened are presented in Table S1). A higher number of cells responded to FsK (70.11%) or Fom (80.95%), compared to *P. indica* exudate (43.59%; Fig. 3a). In addition, although the median number of spikes generated in active cells over 30 minutes of recording was comparable for all exudates (5 peaks for FsK and Fom; 4 peaks for *P. indica*; *p*-value 0.245) (Fig. 3b), when we analysed the distribution of peak numbers among the fungal exudates tested in all cells, we recorded differences among peak numbers generated by *P. indica* and FsK or Fom, respectively (p-value <0.005 for each pairwise comparison). Thus, differences in the pattern of calcium spikes, expressed as the number of spikes per cell over a period were present.

It has been postulated that information in calcium-mediated signals can be encoded in the amplitude and frequency of the spiking, duration of the response as well as tissue specificity, and this information is responsible for the induction of specific responses (McAinsh & Hetherington, 1998) (Vadassery *et al.*, 2009). Thus, we analyzed (Fig. 3c) the oscillatory responses generated by our fungal exudates (Fig. 2) by manually calculating the interval between the treatment and the occurrence of the first spike in active cells (lag phase). Differences in median lag phase values of active cells examined per exudate were sharp (127.96 sec for *P. indica*, 290.32 sec for FsK and 273.12 sec for Fom), and the distribution of lag phase values were statistically different for induced calcium spiking between *P. indica*-FsK and *P. indica*-Fom (p-value <0.005 and p-value <0.05, respectively).

We also measured the width of each spike in all active cells, estimated as the difference in seconds between the first time point of the upward phase (elevation from the baseline - steady state) and the last time point of the downward phase (return to the baseline – steady state) for each spike. Spikes generated by the 3 fungal exudates had comparable median values (60.22 sec for FsK, 63.38 sec for Fom, 66.47 sec for *P. indica;* as calculated in the total number of active cells) (Fig. 3d). Analysis of the distribution of spike width values recorded in response to the three exudates, revealed differences among FsK and *P. indica* (p-value <0.005).

Lastly, we analysed the waiting time, i.e. the interval between subsequent peaks. The histogram in Fig. S5 illustrates the distribution of waiting time autocorrelation values in our populations of spiking profiles. A high number of cells in all treatments demonstrated negative autocorrelation values, indicating that spiking responses to all fungal exudates are in most cases irregular, in analogy to what was described for AM fungal-induced spiking profiles and in contrast with the mostly regular rhizobium-induced calcium spiking signals in the same experimental system (Russo *et al.*, 2013). Statistical analysis showed no dependency between the distribution of waiting time autocorrelation values and the fungal exudate tested.

Altogether our analysis revealed that the conditions (i.e. constituents of the exudates) that determined the distribution of 1) peak number generated over a certain period of time, 2) lag phase prior to spiking initiation, and, 3) peak width of individual traces in response to the 3 elicitors examined, were not the same. *P. indica*- induced calcium spiking had the most profound differences in comparison to *Fusaria*-induced calcium spiking. Pairwise comparison among the two *Fusaria* examined, revealed no differences in any of the parameters examined herein.

Nuclear calcium spiking is abolished in *Mtdmi2-2* but not in *Mtdmi3-1* epidermis

We then extended our investigation of nuclear calcium signals in ROC epidermal cells of mutants for either *MtDMI2 (dmi2-2*) and *MtDMI3* (*dmi3-1*), homologs to *LjSYMRK* and *LjCCAMK,* respectively (Fig. 4, Fig. S6). In *dmi2-2,* very few cells were active in any treatment (10.26% for FsK, 15% for Fom, 3.92 % for *P. indica* exudate). By contrast, nuclear calcium spiking was retained in *dmi3-1* upon stimulation by the fungal exudates tested (Fig. 4a). Furthermore, FsK exudate induced nuclear spiking in a higher percentage of *dmi3-1* cells (81.68%) compared to wt (70.11%). The opposite was observed for Fom exudate (69.70% for *dmi3-1* vs 80.95% for wt), whereas approximately the same percentage of responding cells was recorded in *dmi3-1* and wt treated with *P. indica* exudate (43.50% for *dmi3-1* vs 43.59% for wt) (Fig. 4a).

We then analysed the distribution of peak number in *dmi3-1* cells generated by the three fungal exudates (Fig. 4b). The median number of spikes for active cells was within similar ranges in all exudates (similar median values to those obtained in the wt lines) (Fig. 4b). On the other hand, a significant association was recorded in the peak distribution in total cells (active and non-active) among FsK and *P. indica* exudate (p-value <0.001), indicating again differences in the number of spikes per cell over a period as observed in wt.

In conclusion, all fungal exudates examined generated intense and repeated nuclear calcium oscillations (spiking). Their activation was dependent on *DMI2* (a member of the CSSP acting upstream of calcium oscillations) but not on *DMI3* (acting downstream of calcium signalling), suggesting that the core of the CSSP that transduces AM fungal, rhizobial and actinorrhizal signals (Barker *et al.*, 2017) is also involved in the perception of signals from all three non-mycorrhizal fungi.

The biological activity of *Fusarium* exudates is affected by chitinase and heat treatment

In an attempt to determine the nature of the factors that triggered nuclear calcium spiking by FsK, we hypothesized that if the triggering compounds were chitin-based molecules, their enzymatic cleavage with chitinase would lead to a decrease in the spiking response (Genre *et al.*, 2013) (Chabaud *et al.*, 2016). For this quest, we also included in the analysis the exudates of Fom, since it belongs in the *Fusarium* genus, and the two fungal strains produced similar calcium spiking responses in wt and *dmi3-1* cells. Fig. S7 shows that the percentage of epidermal cells responding to chitinase-treated FsK exudate dropped significantly by 62.86%, and an analogous 44.68% reduction was observed upon chitinase treatment of Fom exudate, compared to their respective control experiments with untreated exudates. As a control for the enzymatic activity of the chitinase solution, we used short-chain COs that are known to elicit calcium spiking in atrichoblasts (Genre *et al.*, 2013). Pre-treatment of 10^{-6} M CO5 with chitinase resulted in partial abolishment of nuclear calcium oscillatory response in our experiments (32.12% reduction; Fig. S8).

As a second step, we examined the stability of the two exudates under heat treatment. To this aim, we autoclaved FsK and Fom exudates at 121°C for 20 min. Again, the reduction in the percent of cells responding to heat-treated exudates as compared to the non-treated ones was more severely affected for FsK (55.92 %) than Fom (14.22 %) (Fig. S7b). A prolonged heat treatment of 60 min did not reduce further the activity of FsK exudates (56.70 % reduction in responding epidermal cells).

In short, our tests suggested that the active molecules present in FsK and Fom exudates include both chitinase- and heat-sensitive compounds. Furthermore, the observed differences in the reduction of the activity between heat-treated FsK and Fom exudates suggests that the molecules that trigger a comparable nuclear calcium spiking pattern are different in the two fungal species.

Reaching the pathway backwards: involvement of LysM-RLKs in *L. japonicus* response

Our results on FRET-based analysis of nuclear calcium changes in wt ROC cells upon chitinase-treated FsK exudate, prompted us to investigate the role of members of the *LysM* RLK gene family in *Lotus*-FsK interaction. We focused on genes that are regulated upon chitin/fungal treatment (Fuechtbauer *et al.*, 2018) (Lohmann *et al.*, 2010) (Rasmussen *et al.*, 2016), and followed their transcriptional regulation over time during *Lotus* root colonization by FsK. More specifically, we investigated the transcript levels of 6 *LjLys* genes: *Lys6*, *Lys11*, *Lys12*, *Lys13*, *Lys14*, *Lys20* (Fig. S9, S2). Four *LysM* genes were transcriptionally regulated during the interaction with FsK: *Lys6* had a statistically significant upregulation (1.5-fold) at 4 dpi, which correlates with maximal fungal presence within plant tissues at this time point (Fig. S2); *Lys13* was upregulated from 2 dpi onwards, and *Lys14* is upregulated only at late stages of the interaction (12 dpi). *Lys12* and *Lys20* expression was not altered in the presence of FsK, while *Lys11* transcript levels were very low in both control and inoculated tissues, under our experimental conditions.

To further investigate the possible role of differentially expressed *LysM* genes in *Lotus*-FsK interaction, we compared FsK colonization levels between wt and mutant lines impaired in *LysM* genes that were also, transcriptionally affected. *Ljlys6-1* displayed significantly higher FsK colonization levels at 4dpi compared to wt plants (Fig. 5a). Since mutant lines for *LjLys13* and *LjLys14* were not available, we opted for the generation of silenced hairy-root lines, to examine the role of these genes in FsK colonization. We introduced an RNA-hairpin construct targeting both *Lys13* and *Lys14* into *L. japonicus* roots, using the *Agrobacterium rhizogenes*-mediated hairy root transformation method. We obtained 7 individual plants showing 70% to 100% reduction in *Lys13* relative transcript levels and 66 to 100% reduction in *Lys14* transcript levels, compared to empty vector-transformed controls (Fig. S10). More specifically, *Lys13* was silenced in all selected plant lines (L3, L11, L14, L17, L26, L27, L47), while only four lines were also silenced for *Lys14* (L11, L17, L27, L47). All *Lys13/14* silenced lines demonstrated statistically significantly lower levels of intraradical FsK colonization when compared to control plants (Fig. 5b, p-value = 0.078). Finally, two more available mutant lines, *Ljlys12-3* and the triple mutant *Ljnfr1nfr5lys11,* were included for comparison, since *Lys12* and *Lys11* expression levels were not affected by the presence of the endophyte. The defect in NF receptors in the triple mutant was not expected to have an effect on FsK colonization. *Ljlys12-3* displayed significantly higher

FsK colonization levels at 4dpi, whereas the triple mutant was colonized to levels similar to those recorded in wt plants (Fig. 5b).

Discussion

Intraradical accommodation of an endophytic fungus is controlled by multiple LysM receptors

Chitin represents the most ancestral structural polysaccharide in the fungal cell wall (Gow *et al.*, 2017), and most fungi possess chitin synthase enzymes. This was recently, also, shown for oomycetes (Fuechtbauer *et al.*, 2018) (Gibelin-Viala *et al.*, 2019), even though their cell walls primarily consist of β-glucans (Mélida *et al.*, 2013). Chitosaccharides of variable degree of polymerization, produced either by enzymatic cleavage of the long crystalline chitin, or synthesized anew, are considered as Microbe Associated Molecular Patterns (MAMPs), able to trigger symbiotic signalling (as is the case of short chain COs) (Genre *et al.*, 2013), or immune responses (as is the case of longer-chain COs, dp = 6–8 N-acetyl glucosamine) (Stacey & Shibuya, 1997) (Kouzai *et al.*, 2014) (Liang *et al.*, 2014). As regards the receptors of chitinaceous signal molecules from symbionts, highly specific ones have been identified for the NF and Myc LCOs (Amor *et al.*, 2003) (Radutoiu *et al.*, 2003) (Limpens *et al.*, 2003) (Madsen *et al.*, 2003) (Maillet *et al.*, 2011) (Fliegmann *et al.*, 2013) (Murakami *et al.*, 2018). Recent work on structurally related molecules from pathogenic fungi has shown that very similar LysM-RLKs in legumes enable discrimination between chitin perception and perception of NFs (Bozsoki *et al.*, 2017).

FsK exudates comprise of, at least partially, chitin-based molecules of unknown degree of polymerization, while heat-labile molecules must also be present. Characterization of the nature of FsK triggering compounds will require substantially additional research but it is notable that heat treatment did not affect the AM fungal exudate activity (Navazio *et al.*, 2007). As anticipated, certain *LysM* genes (*Lys6*, *Lys13*, *Lys14*) are regulated in *Lotus*-FsK interaction, further implying that chitin-based molecules produced by the fungus are recognized by the plant. Two *LysM* genes, *Lys13* and *Lys14* positively control FsK intracellular accommodation and may act as entry receptors of FsK successful passage through the rhizodermis in the legume root. On the contrary, LjLYS6, and perhaps LYS12 may act as balancing receptors, controlling fungal intraradical proliferation, at the post initial infection stages. This role has already been assigned to LYS6 and LYS12 receptors, in interaction of legumes with pathogenic fungi (Bozsoki *et al.*, 2017) (Fuechtbauer *et al.*, 2018).

In the *Lotus*-FsK system, we could detect a phenotype as regards the colonization levels in terms of fungal intraradical accommodation in all available plant lines mutated in *LysM* genes, which are, also, transcriptionally affected by FsK. These RLKs could play a role at both early and late stages of the interaction. Assessing the spatial expression of these genes during FsK progression as well as the putative triggering of immune responses in wt and corresponding mutant lines, will provide further insight in such roles for the accommodation of the endophytic fungus.

A very common symbiosis signalling pathway

Structural similarities between chitin-based elicitors from either symbiotic or non-symbiotic microbes raise questions about how plants distinguish friend from foe (Zipfel & Oldroyd, 2017). We investigated the role of the CSSP in establishing an endophytic association, making use of the *Lotus*-FsK system (Skiada *et al.*, 2019). Our results indicate an unparalleled involvement of the CSSP in *Lotus*-FsK association.

Transcriptional reprogramming of CSSP genes, as well as genes acting downstream of it, have been originally described for RL and AM symbiosis. Apart from symbiotic associations in legumes, the involvement of the CSSP in plant associations has been studied in non-symbiotic bacteria in legumes (Sanchez *et al.*, 2005); in legume-parasitic root-knot nematodes (Weerasinghe *et al.*, 2005); and in the successful nodulation of the actinorrhizal plant *Casuarina glauca* by its symbiont, *Frankia sp.*, in which a functional *Lj*SYMRK (Gherbi *et al.*, 2008) as well as a functional *CCaMK* (Svistoonoff *et al.*, 2013) are required. Recently, *L. japonicus* symbiosis genes were shown to structure the root microbiota, as revealed by CSSP mutant analysis (Thiergart *et al.*, 2019). In our experimental system, among the genes examined, those acting upstream *CCaMK* had no effect on FsK accommodation in *Lotus* roots and were dispensable for determination of FsK colonization levels. In fact, the non-nodulating and non-mycorrhizal *symRK-1* and *castor-1* mutants (Schauser *et al.*, 1998) (Wegel *et al.*, 1998) (Bonfante *et al.*, 2000) (Novero *et al.*, 2002) (Stracke *et al.*, 2002), displayed a wt-like phenotype in terms of intraradical FsK colonization.

The calcium ion is a universal second messenger in numerous plant signalling pathways. Symbiotic calcium spiking lies at the centre of the pathway, downstream the nuclear envelope potassium cation channel(s), which were believed to be CASTOR and POLLUX in *L. japonicus* (Ehrhardt *et al.*, 1996) (Chabaud *et al.*, 2011) (Genre & Russo, 2016). The latter were recently shown to act as highly selective Ca^{2+} channels (Kim *et al.*, 2019), challenging the established knowledge on key players and order of the pathway. Nuclear and perinuclear calcium oscillations

occur also upon perception of Frankia signals by actinorrhizal plants (Chabaud *et al.*, 2016), perception of flagellin (flg22), oligosaccharides and proteins leading to necrosis in *Nicotiana* sp cells (Lecourieux *et al.*, 2005) and upon abiotic stimulation (Lachaud *et al.*, 2010) (van der Luit *et al.*, 1999). Our results show that the exudates of the endophytic FsK trigger periodic calcium oscillations in the nucleus of *M. truncatula* ROCs harbouring nuclear-targeted cameleon reporters (Sieberer *et al.*, 2009). The suppression of this response in *dmi2-2* and its persistence in *dmi3-1* mutants, strongly suggests that FsK-triggered calcium signals are acting within the CSSP, in analogy to what has been observed for the response to AM fungi and rhizobia (Wais *et al.*, 2000) (Chabaud *et al.*, 2011) (Genre *et al.*, 2013). To the best of our knowledge, there are no previous reports of nuclear calcium oscillations upon compatible, non-symbiotic legume-microbe interactions that are CSSP-dependent. *M. truncatula* epidermal cells respond to oomycete cell wall fractions by nuclear calcium oscillations but only in a CSSP-independent manner (Nars *et al.*, 2013). This unprecedented conclusion opens a broad field of discussion about the role of the CSSP outside the restricted group of symbiotic interactions *sensu stricto*.

Indeed, a comparison of nuclear calcium oscillations as a response to FsK exudate with calcium signatures in response to symbiotic factors revealed possible analogies: the patterns recorded in our study resemble those triggered by CO4/AM fungal exudate for their relatively irregular peak distribution. In addition, the average peak width of ~60 sec recorded for FsK, is closer to the 71-100 sec interval for significant peaks in response to Nod factors than to the much shorter 24-36 sec interval observed for mycorrhizal factors (Kosuta *et al.*, 2008). Furthermore, by employing the exudates from two additional fungal species as external controls - the pathogenic *Fusarium oxysporum* f. sp. *medicaginis* and the non-mycorrhizal mutualist *P. indica* - we observed comparable nuclear calcium spiking profiles that are CSSP-dependent.

Generation of nuclear calcium oscillations by multiple fungal strains should not be a surprise. Chitin-based molecules are secreted and/or deposited by fungi at the proximity of the interacting plant cell surface. These molecules are structurally related to rhizobial LCOs, as well as Myc COs/LCOs, which are able to activate nuclear calcium spiking in host plants (Ehrhardt *et al.*, 1996) (Sieberer *et al.*, 2009) (Chabaud *et al.*, 2011). Reported symbiotic calcium spiking inducing signals are therefore primarily chitinaceous and the only currently known exception, to our knowledge, is the case of *Frankia* symbiotic factors able to elicit *NIN* (Nodule Inception) gene activation and nuclear calcium spiking on roots of the actinorrhizal plant *Casuarina glauca*.

Frankia factors are composed of hydrophilic compounds that are resistant to chitinase digestion (Chabaud *et al.*, 2016).

Differences in the spiking profile among the fungal isolates may be attributed to the nature and/or the concentration of the triggering molecules. Despite the fact that both *Fusaria* species as well as the ecological analogue of our strain, the mutualist *P. indica* were routinely cultured in PDA medium, the latter was a relative slow grower (in terms of mycelial growth) in comparison to the other two fungal species. This growth differences might also be reflected in the amount of triggering molecules produced *in vitro,* in the absence of the plant, over the time frame of one week. Furthermore, one would anticipate that closely related fungal species would produce similar triggering molecules, due to cell wall composition similarities. The specificity of nuclear calcium spiking response remains to be verified in planta either in the presence of the exudate or even the fungus itself.

The placement of nuclear calcium spiking at the core of *Lotus*-FsK signalling pathway(s) is supported by CSSP gene expression and phenotyping of mutants impaired in genes acting downstream the nuclear calcium spiking response. *LjCCaMK* (*MtDMI3*) was significantly upregulated both at early and relatively late time points of the interaction. *CCaMK* activation at very early stages of the interaction is of interest, because this gene acts at the core of the signal transduction process. Induction of *CCaMK* at late stages of the interaction, is perhaps associated to fungal progression within host tissues at these stages. Interestingly, *LjCCaMK* expression is only marginally affected by *M. loti* inoculation (Tirichine *et al.*, 2006), suggesting that this calcium-activated enzyme is differentially involved in the two interactions.

An impaired phenotype with lower colonization levels was recorded in both *ccamk-1* and *cyclops-1* mutants, genes acting downstream the calcium spiking response. Interestingly, a comparable delay in nodulation and the occasional and late colonization by AMF (delayed and reduced arbuscule formation) has been reported for the *ccamk-1* weak allele (Schauser *et al.*, 1998) (Demchenko *et al.*, 2004), suggestive of a partial functioning of the truncated protein. Alternatively, at these later time points, and possibly due to fungal overload, the necessity for signal deciphering through CCaMK, and signal transduction through CYCLOPS, may be bypassed by redundant proteins acting in parallel and/or alternative signalling routes that allow the progression of fungal accommodation even in the absence of key components of the CSSP. In this latter case, colonization proceeds fast and reaches wt levels belatedly.

Summarizing the above, we propose that FsK produces at least two different types of molecules to activate the CSSP: chitosaccharides of unknown degree of polymerization, and heat sensitive molecules. FsK colonizes the root of legumes at least via three alternative routes: 1) when all CSSP components are functional, FsK utilizes the pathway by generating nuclear calcium spiking and activating CCaMK; 2) when *SYMRK* is impaired, calcium spiking does not occur, but FsK is still capable of effectively colonizing the root, possibly by activating CCaMK through a SYMRK- and/or calcium spiking-independent route; 3) when the calcium spiking response is generated but cannot be perceived or transmitted (impaired *CCaMK* or *CYCLOPS*) the CSSP is abolished, and yet FsK is still able to colonize the legume root, though with less efficiency. We assume that in this latter case, an unexplored third route allows a less successful intraradical fungal entry (summarized in Figure 6).

Figure 6 is based on the assumption that the CSSP acts in the same manner in both model legumes, in terms of symbiont recognition and subsequent accommodation. The proposed model derived by piecing together results from both plants, due to the availability of genetic tools in each model legume. Based on the recorded FsK-induced, CSSP-dependent nuclear calcium spiking in *M. truncatula* root epidermis, one would anticipate lower colonization levels in mutants of genes acting upstream the calcium spiking response. On the contrary, wt fungal intraradical progression is observed in *symrk* and *castor* mutants, and only *ccamk* and *cyclops* exhibit lower colonization levels. This may be attributed to different modes of action of the same signalling pathway in the two model legumes, supported, for example, by the different number of genes comprising the pathway in the two plant species. Similarly, *cyclops/ipd3* mutants in *L. japonicus/rice* and *M. truncatula* show differences in the AM symbiosis phenotype, indicating that these proteins, or their regulatory context differ within each species (Yano *et al.*, 2008) (Gutjahr *et al.*, 2008) (Horváth *et al.*, 2011) (Ovchinnikova *et al.*, 2011). Furthermore, CSSP mutant alleles of genes acting upstream the Ca^{2+} spiking response, with leaking phenotypes in terms of AM symbiosis, have been identified (Wegel *et al.*, 1998) (Kistner *et al.*, 2005). This, besides the putative partial functioning of the protein, indicates that alternative routes could also be employed by these ancient fungal symbionts when parts of the pathway are impaired or non-functional, or even when the pathway is fully operating (Genre & Russo, 2016). Accordingly, the association of FsK with legumes suggests that proteins could act along a common scaffold (signalling pathway) to mediate the accommodation of other endophytes. In addition, our current knowledge on this common signalling pathway is highly biased by work on legumes. Focusing on non-legume AM hosts could

shed light on this rather unspecified common pathway and could help identify missing steps and intermediates.

By moving 'deeper' into symbiotic signalling, the nodulation- and mycorrhization- specific transcription factors acting downstream the calcium spiking response, *LjNSP1* and *NSP2* (Maillet *et al.*, 2011) (Delaux *et al.*, 2013) were not affected in our system. Nevertheless, CSSP-regulated genes that act early in nodulation process were induced upon FsK interaction. The constant mild induction of *ENOD40* from 4 dpi onwards suggest a possible implication of this nodulin gene in FsK accommodation process. *ENOD40* is an early nodulin gene induced in legume tissues upon NF/chitin pentamer treatment (Minami *et al.*, 1996), during AM infection (van Rhijn *et al.*, 1997) and it is linked to symbiotic (nodule formation) and non-symbiotic organogenetic processes (i.e. lateral root formation) in legumes (Papadopoulou *et al.*, 1996). *ENOD40* is also regulated by cytokinin (van Rhijn *et al.*, 1997). The rapid and sustained expression of *ENOD40* may be linked to the preparation of root tissues for FsK accommodation, i.e. root cell expansion, and perhaps division.

Conclusion

In the present study we have shown that multiple LysM receptors act to allow or balance endophytic, intraradical fungal progression. We further show that the CSSP and more specifically nuclear Ca^{2+} spiking may act as a junction or triggering module for recognition of multiple microbial molecules, whereas in parallel, other molecular players act to discriminate the response. Endophytic progression may, additionally, be controlled at a step post the Ca^{2+} spiking response, and in this scenario, CCaMK activation is partially dispensable. Our results support the emerging notion that the CSSP is not a sole feature of symbiotic interactions of legumes and raise an intriguing question: how legumes utilize one core pathway to discriminate among multiple microbes. Recent reports demonstrate that there is a continuum in plant-microbe interactions; fungal endophytes may occupy different niches or expand their niches. Niche expansion may reflect the endophytes' phylogenetic origin, depend on environmental conditions, (both abiotic and associated microbiome), but also result from co-evolution with their host (Hacquard *et al.*, 2016) (Martino *et al.*, 2018) (Selosse *et al.*, 2018). Focusing on plant-microbe co-evolution, mechanisms that maintain variation for partner quality, a feature essential for the stabilization of symbiosis in

evolutionary terms, are not clearly presented as yet, but it is clear that a dynamic frame of interactions is set (Heath & Stinchcombe, 2014). For example, different plant genotypes may host and respond to the same fungal strain differently, leading either in pathogenicity or benefit (Lofgren *et al.*, 2018) (Suproniene *et al.*, 2019) (Nieva *et al.*, 2019). FsK is capable to achieve entry in the plant, either by use of the CSSP or by an alternative, by-pass pathway, which still allows for a less-successful accommodation of FsK as a beneficial (or at least not harmful) endophyte. The latter may be interpreted in co-evolutionary terms as the opportunity needed for a fungal strain to achieve a better/ best entry strategy within the plant. It also means that slight variations in these early signalling pathways alter the perception of a fungal partner and lead to different plant responses. Our understanding of the importance of these early signalling pathways (currently incompletely understood by analysis of isolated pathways) on determining the final outcome of a plant-fungal association is still limited. Further research is needed to unravel the connection of the perception at the entry points with the downstream responses that may lead to increase fitness of the plant, and such insight may have the potential for practical use.

Acknowledgements

We are grateful to Simona Radutoiu for providing the plant mutant lines; Daniela Tsikou for sharing ideas during the initiation of the project and critical reading of the manuscript; Constantine Garagounis for his contribution in the analysis of hairy roots experiments, and for critical reading of the manuscript; Dimitra Papantoniou for her assistance in the hairy root experiment; Costas Ehaliotis for his suggestions on presentation of Figure 3 and 4. We also thank the three anonymous reviewers for their comments that aid to broaden and improve our manuscript. This work was partially supported by the Postgraduate Programme 3817 of the Department of Biochemistry and Biotechnology, University of Thessaly (to KKP) and Programme 4757.17 (funded by GGSRT/EU/ NSRF to KKP) and COST Action FA1206 and FA1405 (STSM Grants to VS).

Author contributions:

VS: Conceptualization, Resources, Formal analysis, Validation, Investigation, Visualization, Methodology, Writing-original draft; MA: Validation, Investigation, Visualization; PB: Conceptualization, Resources, Supervision, Validation, Methodology, editing; AG: Conceptualization, Resources, Supervision, Validation, Methodology, Writing-review and editing;

KKP: Conceptualization, Resources, Methodology, Validation, Supervision, Funding acquisition, Project administration, Writing-original draft, Writing-review and editing.

References

Amor B Ben, Shaw SL, Oldroyd GED, Maillet F, Penmetsa RV, Cook D, Long SR, Dénarié J, Gough C. **2003**. The NFP locus of *Medicago truncatula* controls an early step of Nod factor signal transduction upstream of a rapid calcium flux and root hair deformation. *Plant Journal* **34**: 495–506.

Antolín-Llovera M, Petutsching EK, Ried MK, Lipka V, Nürnberger T, Robatzek S, Parniske M. **2014**. Knowing your friends and foes - plant receptor-like kinases as initiators of symbiosis or defence. *New Phytologist* **204**: 791–802.

Banhara A, Ding Y, Kühner R, Zuccaro A, Parniske M. **2015**. Colonization of root cells and plant growth promotion by *Piriformospora indica* occurs independently of plant common symbiosis genes. *Frontiers in Plant Science* **6**: 667.

Barker DG, Chabaud M, Russo G, Genre A. **2017**. Nuclear Ca^{2+} signalling in arbuscular mycorrhizal and actinorhizal endosymbioses: on the trail of novel underground signals. *New Phytologist* **214**: 533–538.

Bécard G, Fortin JA. **1988**. Early events of vesicular-arbuscular mycorrhiza formation on Ri T-DNA transformed roots. *New Phytologist* **108**: 211–218.

Bonfante P, Genre A, Faccio A, Martini I, Schauser L, Stougaard J, Webb J, Parniske M.

2000. The *Lotus japonicus LjSym4* gene is required for the successful symbiotic infection of root epidermal cells. *Molecular plant-microbe interactions : MPMI* **13**: 1109–20.

Bozsoki Z, Cheng J, Feng F, Gysel K, Vinther M, Andersen KR, Oldroyd G, Blaise M, Radutoiu S, Stougaard J. **2017**. Receptor-mediated chitin perception in legume roots is functionally separable from Nod factor perception. *Proceedings of the National Academy of Sciences* **114**: E8118–E8127.

Carotenuto G, Chabaud M, Miyata K, Capozzi M, Takeda N, Kaku H, Shibuya N, Nakagawa T, Barker DG, Genre A. **2017**. The rice LysM receptor-like kinase OsCERK1 is required for the perception of short-chain chitin oligomers in arbuscular mycorrhizal signaling. *New Phytologist* **214**: 1440–1446.

Carotenuto G, Volpe V, Russo G, Politi M, Sciascia I, de Almeida-Engler J, Genre A. **2019**. Local endoreduplication as a feature of intracellular fungal accommodation in arbuscular mycorrhizas. *New Phytologist* **223**: 430–446.

Catoira R, Galera C, de Billy F, Penmetsa RV, Journet E-P, Maillet F, Rosenberg C, Cook D, Gough C, Denarie J. **2000**. Four genes of *Medicago truncatula* controlling components of a Nod Factor transduction pathway. *The Plant Cell* **12**: 1647–1665.

Chabaud M, Genre A, Sieberer BJ, Faccio A, Fournier J, Novero M, Barker DG, Bonfante P. **2011**. Arbuscular mycorrhizal hyphopodia and germinated spore exudates trigger Ca^{2+} spiking in the legume and nonlegume root epidermis. *New Phytologist* **189**: 347–355.

Chabaud M, Gherbi H, Pirolles E, Vaissayre V, Fournier J, Moukouanga D, Franche C, Bogusz D, Tisa LS, Barker DG, *et al.* 2016. Chitinase-resistant hydrophilic symbiotic factors secreted by *Frankia* activate both Ca^{2+} spiking and *NIN* gene expression in the actinorhizal plant *Casuarina glauca*. *New Phytologist* **209**: 86–93.

Chabaud M, Venard C, Defaux-Petras A, Becard G, Barker DG. **2002**. Targeted inoculation of *Medicago truncatula* in vitro root cultures reveals *MtENOD11* expression during early stages of infection by arbuscular mycorrhizal fungi. *New Phytologist* **156**: 265–273.

Charpentier M, Bredemeier R, Wanner G, Takeda N, Schleiff E, Parniske M. **2008**. *Lotus japonicus* CASTOR and POLLUX are ion channels essential for perinuclear calcium spiking in legume root endosymbiosis. *The Plant Cell* **20**: 3467–79.

Charpentier M, Oldroyd GED. **2013**. Nuclear calcium signaling in plants. *Plant Physiology* **163**: 496–503.

Cope KR, Bascaules A, Irving TB, Venkateshwaran M, Maeda J, Garcia K, Rush TA, Ma C,

Labbé J, Jawdy S, *et al.* 2019. The ectomycorrhizal fungus *Laccaria bicolor* produces lipochitooligosaccharides and uses the common symbiosis pathway to colonize *Populus* Roots. *The Plant cell* **31**: 2386–2410.

Delaux P-M, Becard G, Combier J-P. **2013**. NSP1 is a component of the myc signaling pathway. *New Phytologist* **199**: 59–65.

Demchenko K, Winzer T, Stougaard J, Parniske M, Pawlowski K. **2004**. Distinct roles of *Lotus japonicus SYMRK* and *SYM15* in root colonization and arbuscule formation. *New Phytologist* **163**: 381–392.

Deshmukh S, Hückelhoven R, Schäfer P, Imani J, Sharma M, Weiss M, Waller F, Kogel K-H. **2006**. The root endophytic fungus *Piriformospora indica* requires host cell death for proliferation during mutualistic symbiosis with barley. *Proceedings of the National Academy of Sciences of the United States of America* **103**: 18450–18457.

Doyle JJ, Doyle JL. **1987**. A rapid DNA isolation procedure for small quantities of fresh leaf tissue. *Phytochemical Bulletin* **19**: 11–15.

Ehrhardt DW, Wais R, Long SR. **1996**. Calcium spiking in plant root hairs responding to rhizobium modulation signals. *Cell* **85**: 673–681.

Ferguson BJ, Mathesius U. **2014**. Phytohormone regulation of legume-rhizobia interactions. *Journal of Chemical Ecology* **40**: 770–790.

Fernandez-Aparicio M, Rispail N, Prats E, Morandi D, Garcia-Garrido JM, Dumas-Gaudot E, Duc G, Rubiales D. **2010**. Parasitic plant infection is partially controlled through symbiotic pathways. *Weed Research* **50**: 76–82.

Fliegmann J, Canova S, Lachaud C, Uhlenbroich S, Gasciolli V, Pichereaux C, Rossignol M, Rosenberg C, Cumener M, Pitorre D, *et al.* 2013. Lipo-chitooligosaccharidic symbiotic signals are recognized by LysM receptor-like kinase LYR3 in the legume *Medicago truncatula*. *ACS Chemical Biology* **8**: 1900–1906.

Franssen HJ, Nap J-P, Gloudemans T, Stiekema W, Van Dam H, Govers F, Louwerse J, Van Kammen A, Bisseling T. **1987**. Characterization of cDNA for nodulin-75 of soybean: a gene product involved in early stages of root nodule development. *Proceedings of the National Academy of Sciences* **84**: 4495–4499.

Fuechtbauer W, Yunusov T, Bozsóki Z, Gavrin A, James EK, Stougaard J, Schornack S, Radutoiu S. **2018**. LYS12 LysM receptor decelerates *Phytophthora palmivora* disease progression in *Lotus japonicus*. *Plant Journal* **93**: 297–310.

Garantonakis N, Pappas ML, Varikou K, Skiada V, Broufas GD, Kavroulakis N, Papadopoulou KK. **2018**. Tomato inoculation with the endophytic strain *Fusarium solani* K results in reduced feeding damage by the zoophytophagous predator *Nesidiocoris tenuis*. *Frontiers in Ecology and Evolution* **6**: 126.

Genre A, Chabaud M, Balzergue C, Puech-Pagès V, Novero M, Rey T, Fournier J, Rochange S, Bécard G, Bonfante P, *et al.* 2013. Short-chain chitin oligomers from arbuscular mycorrhizal fungi trigger nuclear Ca^{2+} spiking in *Medicago truncatula* roots and their production is enhanced by strigolactone. *New Phytologist* **198**: 190–202.

Genre A, Ortu G, Bertoldo C, Martino E, Bonfante P. **2009**. Biotic and abiotic stimulation of root epidermal cells reveals common and specific responses to arbuscular mycorrhizal fungi. *Plant physiology* **149**: 1424–1434.

Genre A, Russo G. **2016**. Does a common pathway transduce symbiotic signals in plant-microbe interactions? *Frontiers in Plant Science* **7**: 96.

Gherbi H, Markmann K, Svistoonoff S, Estevan J, Autran D, Gabor G, Auguy F, Peret B, Laplaze L, Franche C, *et al.* 2008. SymRK defines a common genetic basis for plant root endosymbioses with arbuscular mycorrhiza fungi, rhizobia, and *Frankia* bacteria. *PNAS* **105**: 4928–4932.

Gibelin-Viala C, Amblard E, Puech-Pages V, Bonhomme M, Garcia M, Bascaules-Bedin A, Fliegmann J, Wen J, Mysore KS, le Signor C, *et al.* 2019. The *Medicago truncatula* LysM receptor-like kinase LYK9 plays a dual role in immunity and the arbuscular mycorrhizal symbiosis. *New Phytologist* **223:** 1516-1529.

Glyan'ko AK. **2018**. Phytohormones and morphogenesis of root nodules and lateral roots of a legume plant. *Journal of Stress Physiology & Biochemistry* **14**: 12–26.

Gow NAR, Latge J-P, Munro CA. **2017**. The fungal cell wall: structure, biosynthesis, and function. *Microbiol Spectrum* **5**: FUNK-0035-2016.

Gutjahr C, Banba M, Croset V, An K, Miyao A, An G, Hirochika H, Imaizumi-Anraku H, Paszkowski U. **2008**. Arbuscular mycorrhiza-specific signaling in rice transcends the common symbiosis signaling pathway. *Plant Cell* **20**: 2989–3005.

Hacquard S, Kracher B, Hiruma K, Münch PC, Garrido-Oter R, Thon MR, Weimann A, Damm U, Dallery JF, Hainaut M, *et al.* 2016. Survival trade-offs in plant roots during colonization by closely related beneficial and pathogenic fungi. *Nature Communications* **7**: 11362.

Harris JM, Wais R, Long SR. **2003**. Rhizobium-induced calcium spiking in *Lotus japonicus*.

Molecular plant-microbe interactions : MPMI **16**: 335–341.

Hayes MW, Stutte GW, Mckeon-bennett M, Murray PG. **2014**. Mutualism within a simulated microgravity environment -*Piriformospora indica* promotes the growth of *Medicago truncatula*. *Gravitational and Space Research* **2**: 21–33.

Heath KD, Stinchcombe JR. **2014**. Explaining mutualism variation: a new evolutionary paradox? *Evolution* **68**: 309–317.

Horváth B, Yeun LH, Domonkos Á, Halász G, Gobbato E, Ayaydin F, Miró K, Hirsch S, Sun J, Tadege M, *et al.* 2011. *Medicago truncatula* IPD3 is a member of the common symbiotic signaling pathway required for rhizobial and mycorrhizal symbioses. *Molecular Plant-Microbe Interactions* **24**: 1345–1358.

Huisman R, Bouwmeester K, Brattinga M, Govers F, Bisseling T, Limpens E. **2015**. Haustorium formation in *Medicago truncatula* roots infected by *Phytophthora palmivora* does not involve the common endosymbiotic program shared by arbuscular mycorrhizal fungi and rhizobia. *Molecular Plant-Microbe Interactions* **28**: 1271–1280.

Kalo P, Gleason C, Edwards A, Marsh J, Mitra RM, Hirsch S, Jakab J, Sims S, Long SR, Rogers J, *et al.* 2005. Nodulation signaling in legumes requires NSP2, a member of the GRAS family of transcriptional regulators. *Science* **308**: 1786–1789.

Kavroulakis N, Doupis G, Papadakis IE, Ehaliotis C, Papadopoulou KK. **2018**. Tolerance of tomato plants to water stress is improved by the root endophyte *Fusarium solani* FsK. *Rhizosphere* **6**: 77–85.

Kavroulakis N, Ntougias S, Zervakis GI, Ehaliotis C, Haralampidis K, Papadopoulou KK. **2007**. Role of ethylene in the protection of tomato plants against soil-borne fungal pathogens conferred by an endophytic *Fusarium solani* strain. *Journal of Experimental Botany* **58**: 3853–3864.

Kim S, Zeng W, Bernard S, Liao J, Venkateshwaran M, Ane J-M, Jiang Y. **2019**. Ca^{2+}-regulated Ca^{2+} channels with an RCK gating ring control plant symbiotic associations. *Nature Communications* **10**: 3703.

Kistner C, Winzer T, Pitzschke A, Mulder L, Sato S, Kaneko T, Tabata S, Sandal N, Stougaard J, Webb KJ, *et al.* 2005. Seven *Lotus japonicus* genes required for transcriptional reprogramming of the root during fungal and bacterial symbiosis. *The Plant Cell* **17**: 2217–2229.

Kosuta S, Hazledine S, Sun J, Miwa H, Morris RJ, Downie JA, Oldroyd GED. **2008**. Differential and chaotic calcium signatures in the symbiosis signaling pathway of legumes.

Proceedings of the National Academy of Sciences of the United States of America **105**: 9823–8.

Kouzai Y, Nakajima K, Hayafune M, Ozawa K, Kaku H, Shibuya N, Minami E, Nishizawa Y. **2014**. CEBiP is the major chitin oligomer-binding protein in rice and plays a main role in the perception of chitin oligomers. *Plant Mol Biol* **84**: 519–528.

Krokida A, Delis C, Geisler K, Garagounis C, Tsikou D, Peña-Rodríguez LM, Katsarou D, Field B, Osbourn AE, Papadopoulou KK. **2013**. A metabolic gene cluster in *Lotus japonicus* discloses novel enzyme functions and products in triterpene biosynthesis. *New Phytologist* **200**: 675–690.

Kumagai H, Kinoshita E, Ridge RW, Kouchi H. **2006**. RNAi knock-down of ENOD40s leads to significant suppression of nodule formation in *Lotus japonicus*. *Plant and Cell Physiology* **47**: 1102–1111.

Lace B, Genre A, Woo S, Faccio A, Lorito M, Bonfante P. **2015**. Gate crashing arbuscular mycorrhizas: *in vivo* imaging shows the extensive colonization of both symbionts by *Trichoderma atroviride*. *Environmental Microbiology Reports* **7**: 64–77.

Lachaud C, Da Silva D, Cotelle V, Thuleau P, Xiong TC, Jauneau A, Brière C, Graziana A, Bellec Y, Faure J, *et al.* 2010. Nuclear calcium controls the apoptotic-like cell death induced by d-erythro-sphinganine in tobacco cells. *Cell Calcium* **47**: 92–100.

Lahrmann U, Ding Y, Banhara A, Rath M, Hajirezaei MR, Döhlemann S, von Wirén N, Parniske M, Zuccaro A. **2013**. Host-related metabolic cues affect colonization strategies of a root endophyte. *Proc Natl Acad Sci USA* **110**: 13965–13970.

Lecourieux D, Lamotte O, Bourque S, Wendehenne D, Mazars C, Ranjeva R, Pugin A. **2005**. Proteinaceous and oligosaccharidic elicitors induce different calcium signatures in the nucleus of tobacco cells. *Cell Calcium* **38**: 527–538.

Liang Y, Tóth K, Cao Y, Tanaka K, Espinoza C, Stacey G. **2014**. Lipochitooligosaccharide recognition: an ancient story. *The New phytologist* **204**: 289–296.

Limpens E, Franken C, Smit P, Willemse J, Bisseling T, Geurts R. **2003**. LysM domain receptor kinases regulating rhizobial Nod factor-induced infection. *Science* **302**: 630–633.

Lofgren LA, Leblanc NR, Certano AK, Nachtigall J, Labine KM, Riddle J, Broz K, Dong Y, Bethan B, Kafer CW, *et al.* 2018. *Fusarium graminearum*: pathogen or endophyte of North American grasses? *New Phytologist* **217**: 1203–1212.

Lohmann GV, Shimoda Y, Nielsen MW, Jørgensen FG, Grossmann C, Sandal N, Sørensen K, Thirup S, Madsen LH, Tabata S, *et al.* 2010. Evolution and regulation of the *Lotus japonicus*

LysM receptor gene family. *Molecular Plant-Microbe Interactions* **23**: 510–521.

van der Luit AH, Olivari C, Haley A, Knight MR, Trewavas AJ. **1999**. Distinct calcium signaling pathways regulate calmodulin gene expression in tobacco. *Plant Physiology* **121**: 705 LP – 714.

Madsen EB, Madsen LH, Radutoiu S, Olbryt M, Rakwalska M, Szczyglowski K, Sato S, Kaneko T, Tabata S, Sandal N, *et al.* 2003. A receptor kinase gene of the LysM type is involved in legume perception of rhizobial signals. *Nature* **425**: 637–640.

Maekawa T, Kusakabe M, Shimoda Y, Sato S, Tabata S, Murooka Y, Hayashi M. **2008**. Polyubiquitin promoter-based binary vectors for overexpression and gene silencing in *Lotus japonicus*. *Molecular Plant-Microbe Interactions* **21**: 375–382.

Maillet F, Poinsot V, André O, Puech-Pagès V, Haouy A, Gueunier M, Cromer L, Giraudet D, Formey D, Niebel A, *et al.* 2011. Fungal lipochitooligosaccharide symbiotic signals in arbuscular mycorrhiza. *Nature* **469**: 58–63.

Martino E, Morin E, Grelet GA, Kuo A, Kohler A, Daghino S, Barry KW, Cichocki N, Clum A, Dockter RB, *et al.* 2018. Comparative genomics and transcriptomics depict ericoid mycorrhizal fungi as versatile saprotrophs and plant mutualists. *New Phytologist* **217**: 1213–1229.

McAinsh MR, Hetherington AM. **1998**. Encoding specificity in Ca^{2+} signalling systems. *Trends in Plant Science* **3**: 32–36.

Mélida H, Sandoval-Sierra J V., Diéguez-Uribeondo J, Bulone V. **2013**. Analyses of extracellular carbohydrates in oomycetes unveil the existence of three different cell wall types. *Eukaryotic Cell* **12**: 194–203.

Minami E, Kouchi H, Cohn JR, Ogawa T, Stacey G. **1996**. Expression of the early nodulin, ENOD40, in soybean roots in response to various lipo-chitin signal molecules. *Plant Journal* **10**: 23–32.

Miwa H, Sun J, Oldroyd GED, Downie JA. **2006**. Analysis of Nod-factor-induced calcium signaling in root hairs of symbiotically defective mutants of *Lotus japonicus*. *Molecular plant-microbe interactions : MPMI* **19**: 914–923.

Miyawaki A, Llopis J, Heim R, McCaffery JM, Adams JA, Ikura M, Tsien RY. **1997**. Fluorescent indicators for Ca^{2+} based on green fluorescent proteins and calmodulin. *Nature* **388**: 882–887.

Murakami E, Cheng J, Gysel K, Bozsoki Z, Kawaharada Y, Hjuler CT, Sørensen KK, Tao K, Kelly S, Venice F, *et al.* 2018. Epidermal LysM receptor ensures robust symbiotic signalling in

Lotus japonicus. *eLife* **7**: e33506.

Nars A, Lafitte C, Chabaud M, Drouillard S, Melida H, Danoun S, Le Costaouec T, Rey T, Benedetti J, Bulone V, *et al.* 2013. *Aphanomyces euteiches* cell wall fractions containing novel glucan-chitosaccharides induce defense genes and nuclear calcium oscillations in the plant host *Medicago truncatula*. *PLoS ONE* **8**: e75039.

Navazio L, Moscatiello R, Genre A, Novero M, Baldan B, Bonfante P, Mariani P. 2007. A diffusible signal from arbuscular mycorrhizal fungi elicits a transient cytosolic calcium elevation in host plant cells. *Plant Physiology* **144**: 673 LP – 681.

Nieva AS, Vilas JM, Gárriz A, Maiale SJ, Menéndez AB, Erban A, Kopkac J, Ruiz OA. 2019. The fungal endophyte *Fusarium solani* provokes differential effects on the fitness of two *Lotus* species. *Plant Physiology and Biochemistry* **144**: 100–109.

Novero M, Faccio A, Genre A, Stougaard J, Webb KJ, Mulder L, Parniske M, Bonfante P. 2002. Dual requirement of the *LjSym4* gene for mycorrhizal development in epidermal and cortical cells of *Lotus japonicus* roots. *New Phytologist* **154**: 741–749.

Ovchinnikova E, Journet EP, Chabaud M, Cosson V, Ratet P, Duc G, Fedorova E, Liu W, Op Den Camp R, Zhukov V, *et al.* 2011. IPD3 controls the formation of nitrogen-fixing symbiosomes in pea and *Medicago* spp. *Molecular Plant-Microbe Interactions* **24**: 1333–1344.

Papadopoulou K, Roussis A, Katinakis P. 1996. *Phaseolus* ENOD40 is involved in symbiotic and non-symbiotic organogenetic processes: Expression during nodule and lateral root development. *Plant Molecular Biology* **30**: 403–417.

Pappas ML, Liapoura M, Papantoniou D, Avramidou M, Kavroulakis N, Weinhold A, Broufas GD, Papadopoulou KK. 2018. The beneficial endophytic fungus *Fusarium solani* strain K alters tomato responses against spider mites to the benefit of the plant. *Frontiers in Plant Science* **9**: 1603.

Parniske M. 2008. Arbuscular mycorrhiza: the mother of plant root endosymbioses. *Nature Reviews Microbiology* **6**: 763.

Radutoiu S, Madsen LH, Madsen EB, Felle HH, Umehara Y, Grønlund M, Sato S, Nakamura Y, Tabata S, Sandal N, *et al.* 2003. Plant recognition of symbiotic bacteria requires two LysM receptor-like kinases. *Nature* **425**: 585–592.

Ramírez-Suero M, Khanshour A, Martinez Y, Rickauer M. 2010. A study on the susceptibility of the model legume plant *Medicago truncatula* to the soil-borne pathogen *Fusarium oxysporum*. *European Journal of Plant Pathology* **126**: 517–530.

Rasmussen SR, Füchtbauer W, Novero M, Volpe V, Malkov N, Genre A, Bonfante P, Stougaard J, Radutoiu S. **2016**. Intraradical colonization by arbuscular mycorrhizal fungi triggers induction of a lipochitooligosaccharide receptor. *Scientific Reports* **6**: 1–12.

van Rhijn P, Fang Y, Galili S, Shaul O, Atzmon N, Wininger S, Eshed Y, Lum M, Li Y, To V, *et al.* 1997. Expression of early nodulin genes in alfalfa mycorrhizae indicates that signal transduction pathways used in forming arbuscular mycorrhizae and rhizobium-induced nodules may be conserved. *Proceedings of the National Academy of Sciences of the United States of America* **94**: 5467–5472.

Russo G, Spinella S, Sciacca E, Bonfante P, Genre A. **2013**. Automated analysis of calcium spiking profiles with CaSA software: two case studies from root-microbe symbioses. *BMC plant biology* **13**: 224.

Sanchez L, Weidmann S, Arnould C, Bernard AR, Gianinazzi S, Gianinazzi-Pearson V. **2005**. *Pseudomonas fluorescens* and *Glomus mosseae* trigger *DMI3*-dependent activation of genes related to a signal transduction pathway in roots of *Medicago truncatula*. *Plant Physiology* **139**: 1065 LP – 1077.

Schauser L, Handberg K, Sandal N, Stiller J, Thykjaer T, Pajuelo E, Nielsen A, Stougaard J. **1998**. Symbiotic mutants deficient in nodule establishment identied after T-DNA transformation of *Lotus japonicus*. *Mol Gen Genet* **259**: 414–423.

Selosse MA, Schneider-Maunoury L, Martos F. **2018**. Time to re-think fungal ecology? Fungal ecological niches are often prejudged. *New Phytologist* **217**: 968–972.

Sieberer BJ, Chabaud M, Timmers AC, Monin A, Fournier J, Barker DG. **2009**. A nuclear-targeted cameleon demonstrates intranuclear Ca^{2+} spiking in *Medicago truncatula* root hairs in response to rhizobial nodulation factors. *Plant Physiology* **151**: 1197–1206.

Skiada V, Faccio A, Kavroulakis N, Genre A, Bonfante P, Papadopoulou KK. **2019**. Colonization of legumes by an endophytic *Fusarium solani* strain FsK reveals common features to symbionts or pathogens. *Fungal Genetics and Biology* **127**: 60–74.

Snyder WC, Hansen HN. **1940**. The species concept in *Fusarium*. *American Journal of Botany* **27**: 64–67.

Stacey G, Shibuya N. **1997**. Chitin recognition in rice and legumes. *Plant and Soil* **194**: 161–169.

Stracke S, Kistner C, Yoshida S, Mulder L, Sato S, Kaneko T, Tabata S, Sandal N, Stougaard J, Szczyglowski K, *et al.* 2002. A plant receptor-like kinase required for both bacterial and fungal symbiosis. *Nature* **417**: 959–962.

Sun J, Miller JB, Granqvist E, Wiley-Kalil A, Gobbato E, Maillet F, Cottaz S, Samain E, Venkateshwaran M, Fort S, *et al.* 2015. Activation of symbiosis signaling by arbuscular mycorrhizal fungi in legumes and rice. *The Plant cell* **27**: 823–38.

Suproniene S, Kadziene G, Irzykowski W, Sneideris D, Ivanauskas A, Sakalauskas S, Serbiak P, Svegzda P. **2019**. Asymptomatic weeds are frequently colonised by pathogenic species of *Fusarium* in cereal-based crop rotations. *Weed Research*: 312–323.

Svistoonoff S, Benabdoun FM, Nambiar-Veetil M, Imanishi L, Vaissayre V, Cesari S, Diagne N, Hocher V, de Billy F, Bonneau J, *et al.* 2013. The independent acquisition of plant root nitrogen-fixing symbiosis in Fabids recruited the same genetic pathway for nodule organogenesis. *PLOS ONE* **8**: e64515.

Takeda N, Okamoto S, Hayashi M, Murooka Y. **2005**. Expression of *LjENOD40* genes in response to symbiotic and non-symbiotic signals: *LjENOD40-1* and *LjENOD40-2* are differentially regulated in *Lotus japonicus*. *Plant and Cell Physiology* **46**: 1291–1298.

Thiergart T, Zgadzaj R, Bozsoki Z, Garrido-Oter R, Radutoiu S, Schulze-Lefert P. **2019**. *Lotus japonicus* symbiosis genes impact microbial interactions. *mBio* **10**: e01833-19.

Tirichine L, Imaizumi-Anraku H, Yoshida S, Murakami Y, Madsen LH, Miwa H, Nakagawa T, Sandal N, Albrektsen AS, Kawaguchi M, *et al.* 2006. Deregulation of a Ca^{2+}/calmodulin-dependent kinase leads to spontaneous nodule development. *Nature* **441**: 1153–6.

Vadassery J, Ranf S, Drzewiecki C, Mithofer A, Mazars C, Scheel D, Lee J, Oelmu R. **2009**. A cell wall extract from the endophytic fungus *Piriformospora indica* promotes growth of *Arabidopsis* seedlings and induces intracellular calcium elevation in roots. *The Plant Journal* **59**: 193–206.

Verma S, Varma A, Rexer K, Hassel A, Kost G, Sarbhoy A, Bisen P, Butehorn B, Franken P. **1998**. *Piriformospora indica*, gen. et sp. nov., a new root-colonizing fungus. *Mycologia* **90**: 896–903.

Wais RJ, Galera C, Oldroyd G, Catoira R, Penmetsa R V, Cook D, Gough C, Denarié J, Long SR. **2000**. Genetic analysis of calcium spiking responses in nodulation mutants of *Medicago truncatula*. *Proceedings of the National Academy of Sciences of the United States of America* **97**: 13407–13412.

Wang E, Schornack S, Marsh JF, Gobbato E, Schwessinger B, Eastmond P, Schultze M, Kamoun S, Oldroyd GED. **2012**. A common signaling process that promotes mycorrhizal and oomycete colonization of plants. *Current Biology* **22**: 2242–2246.

Weerasinghe RR, Bird DM, Allen NS. **2005**. Root-knot nematodes and bacterial Nod factors elicit common signal transduction events in *Lotus japonicus*. *Proceedings of the National Academy of Sciences* **102**: 3147–3152.

Wegel E, Schauser L, Sandal N, Stougaard J, Parniske M. **1998**. Mycorrhiza mutants of *Lotus japonicus* define genetically independent steps during symbiotic infection. *Molecular Plant-Microbe Interactions* **11**: 933–936.

van de Wiel C, Scheres B, Franssen H, van Lierop MJ, van Lammeren A, van Kammen A, Bisseling T. **1990**. The early nodulin transcript ENOD2 is located in the nodule parenchyma (inner cortex) of pea and soybean root nodules. *The EMBO Journal* **9**: 1–7.

Yano K, Yoshida S, Mueller J, Singh S, Banba M, Vickers K, Markmann K, White C, Schuller B, Sato S, *et al.* 2008. CYCLOPS, a mediator of symbiotic intracellular accommodation. *Proceedings of the National Academy of Sciences of the United States of America* **105**: 20540–20545.

Zgadzaj R, James EK, Kelly S, Kawaharada Y, de Jonge N, Jensen DB, Madsen LH, Radutoiu S. **2015**. A legume genetic framework controls infection of nodules by symbiotic and endophytic bacteria. *PLoS Genetics* **11**: 1–21.

Zipfel C, Oldroyd GED. **2017**. Plant signalling in symbiosis and immunity. *Nature* **543**: 328.

Supporting Information

Methods S1 Supporting information on materials and methods used in the present study.

Figure S1 Relative expression of *L. japonicus* genes acting within and downstream the CSSP, upon FsK treatment**.**

Figure S2 Heatmap summarizing fold-changes in relative transcript levels of genes examined in the present study.

Figure S3 Changes in CFP, YFP fluorescence over time obtained from *M. truncatula* wt ROC epidermal cells upon elicitation with fungal exudates.

Figure S4 Absence of calcium spiking in response to mock treatment, and generation of calcium spiking in response to CO5 and *G. margarita* germinated spore exudate treatment.

Figure S5 Distribution of waiting time autocorrelation values in the spiking profiles induced by fungal exudates.

Figure S6 Nuclear calcium spiking is abolished in the *M. truncatula dmi2-2*, but maintained in the *Mt dmi3-1* mutant lines.

Figure S7 Nuclear calcium spiking responses in *M. truncatula* wt ROCs elicited by FsK/Fom fungal exudate pretreated with chitinase or heat.

Figure S8 Partial abolishment of nuclear calcium spiking in *M. truncatula* wt ROC epidermis upon chitinase treatment of chitooligosaccharides.

Figure S9 Temporal gene expression analysis of *L. japonicus LysM* genes upon FsK treatment.

Figure S10 Verification of *L. japonicus Lys13* and/or *Lys14* gene silencing in *Lys13*/*14* RNAi lines.

Table S1 Summary of individual *M. truncatula* ROC segments (biological replicates), total plant cell nuclei, and total number of peaks screened for the measurements presented.

Table S2 Primer sequences used in the present work.

Figure legends

Figure 1 Quantification of *Fusarium solani* strain K (FsK) colonization in *Lotus japonicus* common symbiotic signalling pathway (CSSP) mutants.

Absolute quantification of FsK ingress within *L. japonicus* root tissues in wild-type (wt) and CSSP mutants (*symRK-1*, *castor-1*, *ccamK-1*, *cyclops-1*), via qPCR, using primers specific for a fragment of *Fusarium ITS* gene. Tissues were harvested at 4 and 8days post inoculation (dpi). *ITS* gene copy numbers are normalized to ng of total DNA extracted from the root tissue. Data are presented as a dotplot in combination with a boxplot. Each dot represents a single biological replicate. Five (5) biological replicates were assessed for each genotype. Each replicate consists of 3 individual plants. Boxplots extend from the 25th to 75th percentile, respectively. The midline indicates the median of the distribution (red line). Whiskers go down to the smallest value and up to the largest, thus showing all data points. Average values are presented as a red asterisk. Note that outliers are presented as blue triangles. Outliers were not removed from subsequent analysis, as they were considered result of biological variability within the system.

The experiment was repeated twice with similar results.

Black asterisks represent statistically significant differences between wt and the respective mutant line at the 0.05 level (Student's t-test).

Figure 2 Exudates produced by fungi induce changes in nuclear calcium levels imaged using cameleon *Medicago truncatula* (*Mt*) root organ cultures (ROCs).

Calcium spiking responses were recorded in a low-trichoblast-region located 10-20 mm from the root tip. *M. truncatula* wild-type (wt) ROCs expressing the NupYC2.1 cameleon were used for the bioassay. Fungal exudates derived from *Fusarium solani* strain K (FsK), *F. oxysporum* f. sp. *medicaginis* (Fom), or *Piriformospora indica* were used as elicitors.

Representative plots showing changes in nuclear calcium levels after treatment with 10x concentrated FsK, Fom, or *P. indica* exudate, in a 30 min recording. Graphs show ratios of Yellow Fluorescent Protein (YFP) to Cyan Fluorescent Protein (CFP) fluorescence over time. The respective changes in fluorescence over time are presented in graphs of Supporting Information Figure S3.

Figure 3 Analysis of fungal exudate-triggered nuclear calcium responses in *Medicago truncatula* wild-type (wt) root organ cultures (ROCs) epidermis.

Calcium spiking responses were recorded in a low-trichoblast-region located 10-20 mm from the root tip. *M. truncatula* wt (ROCs) expressing the NupYC2.1 cameleon were used for the bioassay. Fungal exudates derived from *Fusarium solani* strain K (FsK), *F. oxysporum* f. sp. *medicaginis* (Fom), or *Piriformospora indica* were used as elicitors.

(a) Percentage of responsive cells (peak number>2), in 30 min recordings post fungal exudate application. Data are presented as a dotplot in combination with a boxplot for each exudate. Each dot represents a single biological replicate (individual lateral root segments derived from ROCs). Boxplots extend from the 25th to 75th percentile, respectively. The midline indicates the median of the distribution (red line). Whiskers go down to the smallest value and up to the largest, thus showing all data points. Average values are presented as a red asterisk. No statistically significant difference was recorded in average percentages of cells showing calcium spikes in response to FsK/Fom/*P. indica* exudate elicitation (one-way anova).

(b) Histogram exhibiting the distribution of fungal exudate-induced calcium spiking responses in all nuclei examined (active and non-active cells). Dots represent the frequency of peak number (presented in continuous intervals of 1 peak) in a 30 min recording period. Median peak number values calculated only in active cells are also presented in red.

Two-sample Kolmogorov Smirnov (K-S) test was performed to compare the distribution of peak numbers generated in response to the three exudates. Distributions were compared in a pairwise manner, under the null hypothesis that populations are drawn from the same distribution. When all cells (active and non-active) were included in the analysis: FsK-*P. indica* and Fom-*P. indica* comparison showed that data are drawn from different distributions ($p<0.005$ for both comparisons).

(c) Cumulative probability line plots showing, for each exudate (depicted by different line colour), the percentage of active cells as functions of the delay time (in sec) recorded prior to spiking initiation. Lag phases were measured manually for all active nuclei examined per elicitor. Lag phase represents the time intervening between the recording initiation and the first recorded spike for each responsive nucleus. Median delay time values are also presented in red.

Two-sample K-S test was performed to compare the distribution of lag phases recorded in response to each elicitor. Distributions were compared in a pairwise manner, under the null hypothesis that populations are drawn from the same distribution. Pairwise comparisons among FsK-*P. indica* and Fom-*P. indica* showed that data are drawn from different distributions ($p<0.005$ and $p<0.05$, respectively).

(d) Cumulative probability line plots showing, for each elicitor (depicted by different line colour), the percentage of active cells as functions of the spike width (in sec). Spike widths were measured manually for all peaks recorded and for each fungal exudate applied. Median spike width values are also presented in red.

Two-sample K-S test was performed to compare the distribution of spike width values recorded in response to each elicitor. Distributions were compared in a pairwise manner, under the null hypothesis that populations are drawn from the same distribution. Pairwise comparisons among FsK-*P. indica* showed that data are drawn from different distributions ($p<0.005$).

Light grey/dark grey/black lines in panels (b), (c), (d): frequencies for FsK/Fom/*P. indica* exudate-elicited calcium spiking responses, respectively.

The number of biological replicates/nuclei/peaks assessed for each elicitor and for each analysis is indicated in Supporting Information Table S1.

Figure 4 Analysis of fungal exudate-triggered nuclear calcium responses in *Medicago truncatula dmi2-2* and *dmi3-1* root organ cultures (ROCs) epidermis.

Calcium spiking responses in a low-trichoblast-region located 10-20 mm from the root tip. *M. truncatula dmi2-2* and *dmi3-1* mutant lines (ROCs) expressing the NupYC2.1 cameleon were used for the bioassay. Fungal exudates derived from *Fusarium solani* strain K (FsK), *F. oxysporum* f. sp. *medicaginis* (Fom), or *Piriformospora indica* were used as elicitors.

(a) Percentage of responsive cells (peak number>2) in the *dmi2-2* and *dmi3-1* mutant background, in 30 min recordings. Data are presented as a dotplot in combination with a boxplot for each mutant line/exudate. Each dot represents a single biological replicate (individual lateral root segments derived from ROCs). Boxplots extend from the 25th to 75th percentile, respectively. The midline indicates the median of the distribution (red line). Whiskers go down to the smallest value and up to the largest, thus showing all data points. Average values are presented as a red asterisk. Note that an outlier is presented in *dmi3-1* lines for Fom exudate (presented as a blue triangle). Outlier value was included in the analysis, as it was considered result of biological variability within the system.

Different letters indicate statistically significant differences in percentages of *dmi3-1* responding cells to each elicitor (one-way anova performed in biological replicates, followed by Tukey's post-hoc test).

(b) Histogram exhibiting the distribution of fungal exudate-induced calcium spiking responses in nuclei of *dmi3-1* ROC segments (active and non-active cells). Dots represent the frequency of peak number (presented in continuous intervals of 1 peak) in a 30 min recording period. Median peak number values calculated only in only active cells are presented in red.

Two-sample (K-S) test was performed to compare the distribution of peak numbers generated in response to fungal exudates. Distributions were compared in a pairwise manner, under the null hypothesis that populations are drawn from the same distribution. When all cells (active and non-active) were included in the analysis, FsK-*P. indica* comparison showed that data are drawn from different distributions ($p<0.001$).

Light grey/dark grey/black lines: frequencies of peak number values of FsK/Fom/*P. indica* exudate-elicited calcium spiking responses in panel (b), respectively.

The number of biological replicates/nuclei assessed for each elicitor/ROC line is indicated in Supporting Information Table S1.

Figure 5 Quantification of *Fusarium solani* strain K (FsK) abundance in roots of *Lotus japonicus* mutants impaired in Lysin-motif (*LysM*) receptors, and in *LysM13*/*14* RNAi lines.

(a) Absolute quantification of FsK ingress within *L. japonicus* root tissues in wild-type (wt) and *LysM* mutants (*lys6-1, nfr1nfr5lys11, lys12-3*), via qPCR, using primers specific for a fragment of *Fusarium ITS* gene. Tissues were harvested at 4 days post inoculation (dpi). *ITS* gene copy numbers are normalized to ng of total DNA extracted from wt and mutant root tissues, respectively. Five (5) biological replicates were assessed for each genotype. Each replicate consists of 3 individual plants. Data are presented as a dotplot in combination with a boxplot. Each dot represents a single biological replicate. Boxplots extend from the 25th to 75th percentile, respectively. The midline indicates the median of the distribution (red line). Whiskers go down to the smallest value and up to the largest, thus showing all data points. Average values are presented as a red asterisk. Note that outlier values are presented as blue triangles. Outlier values were included in subsequent analysis, as they were considered result of biological variation within the system.

Black asterisks represent statistically significant differences between wt and the respective mutant lines at the 0.05 level (Student's t-test).

(b) Absolute quantification of FsK abundance within control lines (presented as average values of 4 independent plants) transformed with an empty T-DNA vector, and within 7 independent hairy

root lines transformed with a *Lys13*/*14* RNAi silencing construct (L3-L47). Quantification was performed via qPCR, using primers specific for a fragment of *Fusarium TEF1a* gene. Tissues were harvested at 5 dpi. *TEF1a* gene copy numbers are normalized to ng of total DNA extracted from each root tissue sample.

Data are presented as a dotplot. For the control, each dot represents a single biological replicate. Median value is presented in red. Each replicate consists of an individual plant. Four (4) independent plants were assessed. For the *LysM13*/*14* RNAi lines, each dot represents the mean of 2 technical replicates.

Mean FsK abundance value (average *TEF1a* gene copy numbers) of all *Lys13*/*14* RNAi lines is significantly lower than that of controls at the 0.05 level (Student's t-test).

The % reduction in *Lys13* or *Lys14* relative transcript levels in RNAi lines in comparison to relative transcript levels in controls (as quantified via gene expression analysis; presented in Supporting Information Figure S10) is presented at the lower part of the graph.

The black asterisk represents statistically significant difference between wt and RNAi lines at the 0.05 level (Student's t-test).

n.r., no reduction in respective relative transcript levels.

Figure 6 Schematic summary describing putative recognition events of *Fusariun solani* strain K (FsK) by *Lotus japonicus* root cells, signalling cascade, and subsequent fungal accommodation.

(a) A chitin-based molecule - perhaps chitooligosaccharides (COs) of unknown degree of polymerization - is recognized by plasma membrane-located Lysin-motif (LysM) – receptor like kinases (RLK(s)), or a heat labile molecule (asterisk) is recognized by an RLK. SYMRK is activated, and signalling through the common symbiotic signalling (CSSP) leads to calcium influx in the nucleoplasm. Calcium spiking occurs in the nucleoplasm, the generated signal is perceived through CCaMK and transmitted through CYCLOPS phosphorylation. Downstream activation of symbiosis genes (like *ENOD40*) occurs. Fungal accommodation progresses normally.

(b) When SYMRK is impaired, calcium spiking does not occur in the nucleus. Recognition of triggering molecules by LysM-RLK(s) leads to a SYMRK- and calcium-independent activation of CCaMK. This SYMRK-independent activation of CCaMK allows an 'on time' fungal progression at wild-type (wt) levels. Activation of ENOD40 perhaps occurs as in the wt.

(c) When CCaMK is impaired, the calcium signal cannot be perceived or transmitted (i.e. when

CYCLOPS is impaired). Activation of SYMRK occurs normally, calcium influx occurs in the nucleus and calcium spiking is generated. The pathway downstream CCaMK is not utilized. A different pathway is activated which may still employ certain components of the symbiosis pathway. Fungal accommodation progresses belatedly, indicating that CCaMK is at the core of FsK recognition pathway in legumes.

Uncertainties in the pathway, and possible parallel/alternative routes are demonstrated with arrows in red.

The scheme was conceptualized by piecing together results derived from (1) *L. japonicus* mutant analysis, and (2) calcium spiking analysis in *Medicago truncatula* root organ cultures.

Root tissues are drawn in brown, whereas the fungus is drawn in yellow.

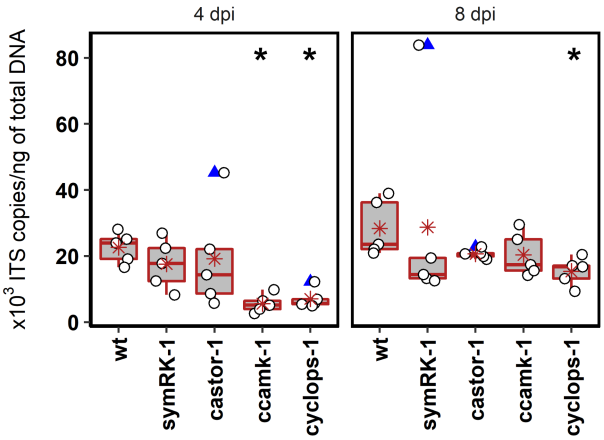

nph_16457_f1.png

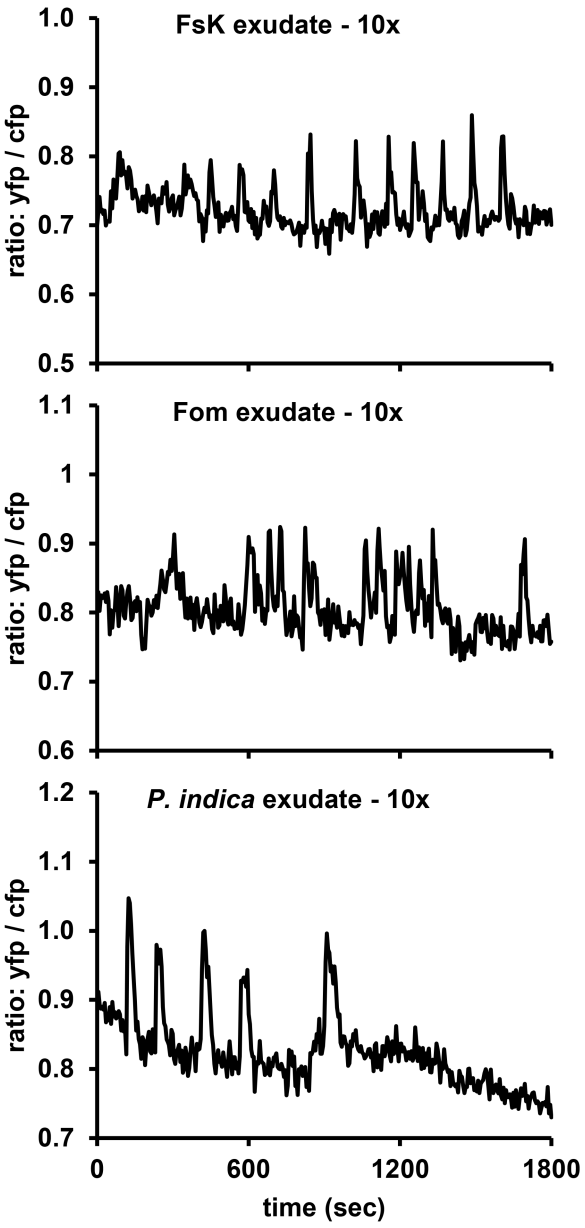

nph_16457_f2.tif

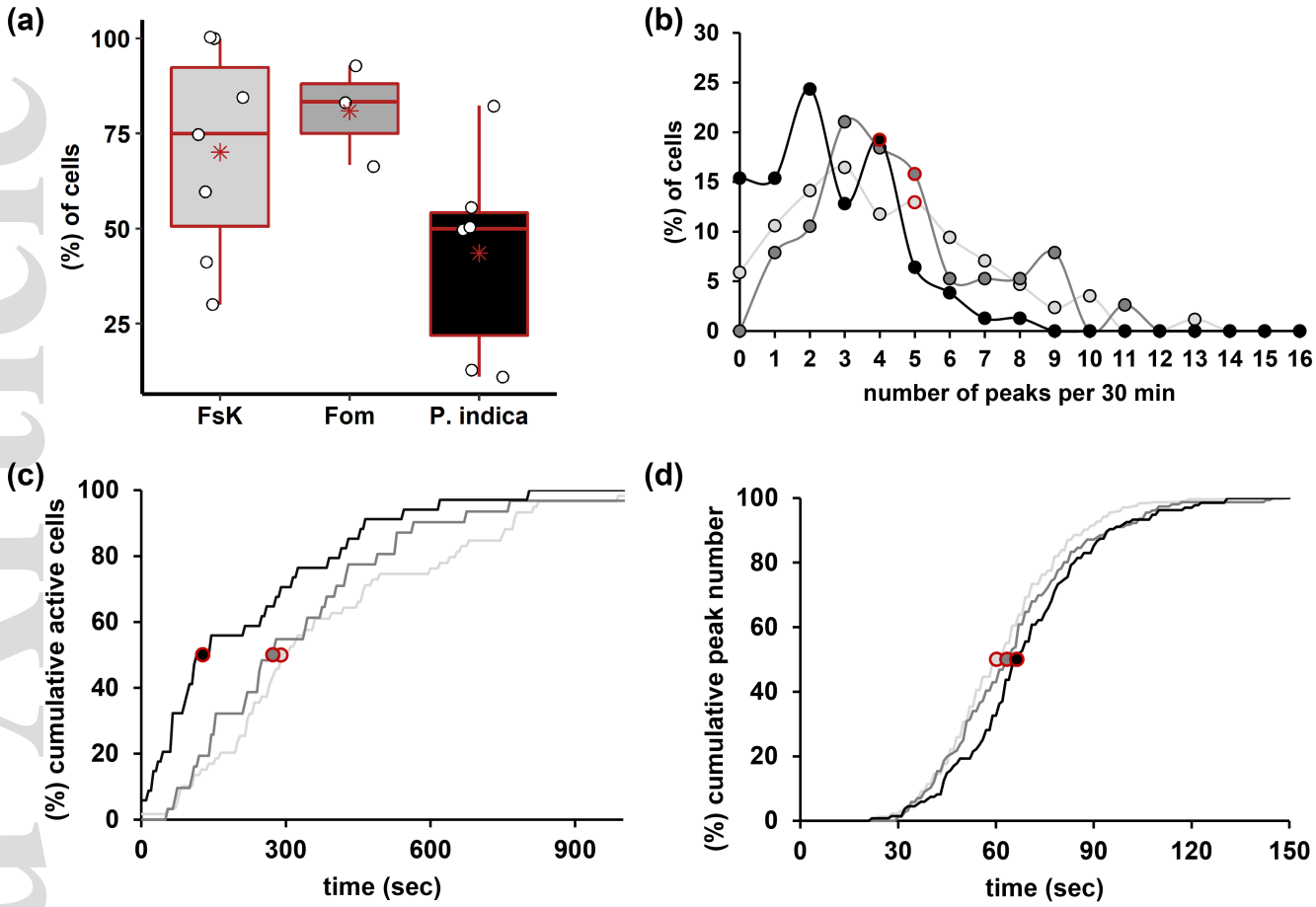

nph_16457_f3.tif

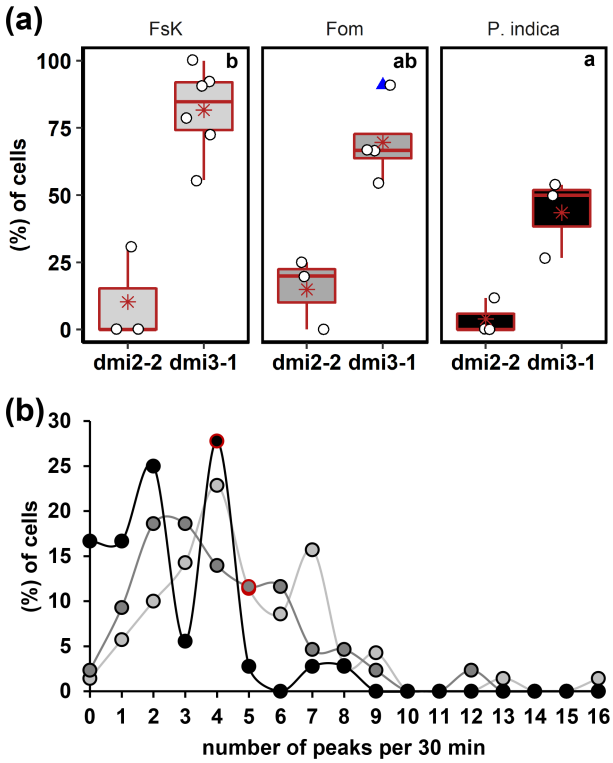

nph_16457_f4.tif

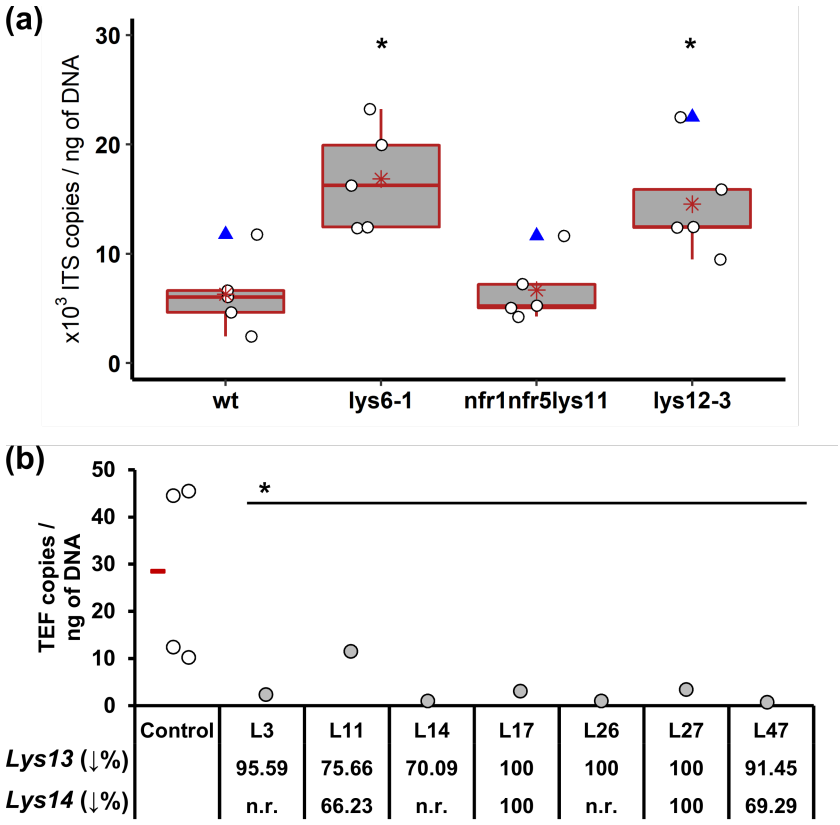

nph_16457_f5.png

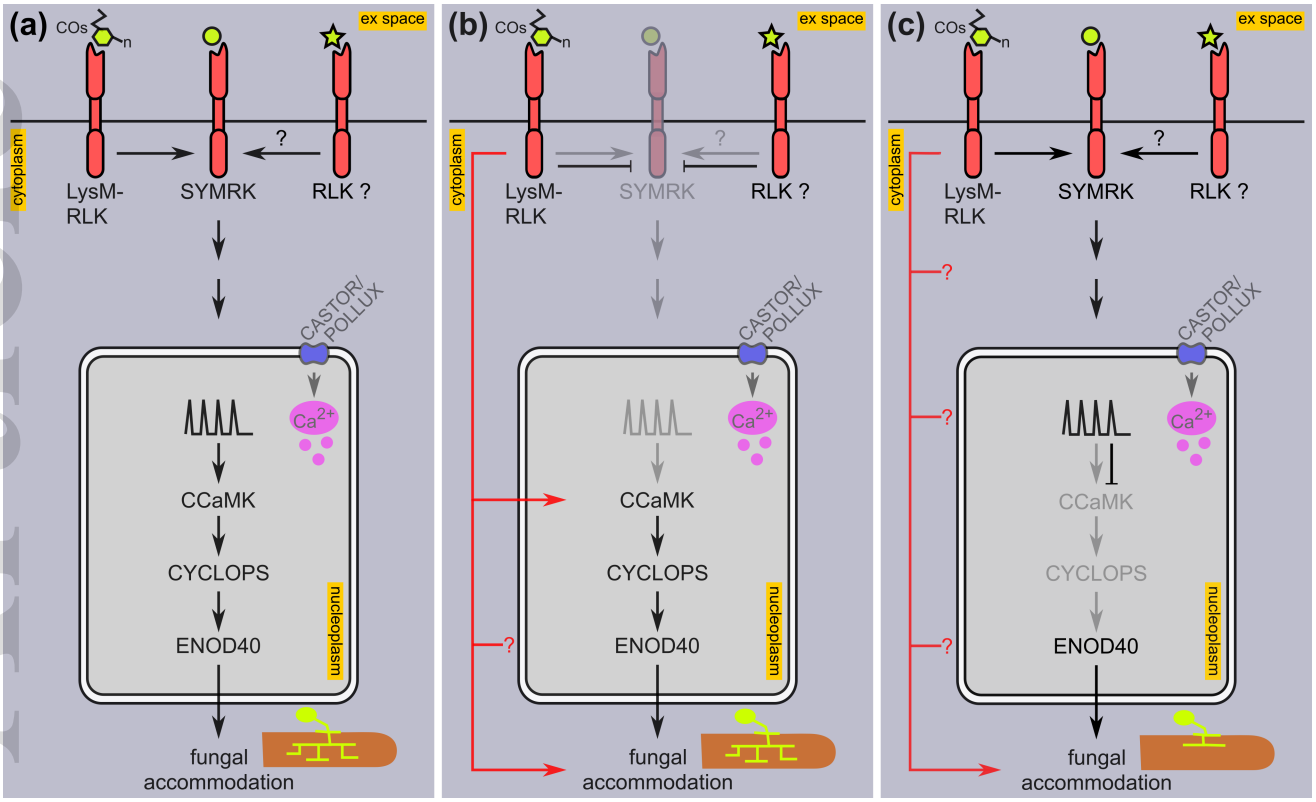

nph_16457_f6.png